VILNIUS UNIVERSITY

CENTER FOR PHYSICAL SCIENCES AND TECHNOLOGY

ALDONA BALČIŪNAITĖ

NEW MATERIALS FOR ALKALINE FUEL CELLS: SYNTHESIS, CHARACTERIZATION AND PROPERTIES

Summary of doctoral dissertation

Physical Sciences, Chemistry (03 P)

Vilnius 2017

The dissertation has been prepared at the Department of Catalysis of Center for Physical Sciences and Technology during the period of 2012 - 2016.

Scientific supervisor: Dr. L.Tamašauskaitė-Tamašiūnaitė (Center for Physical Sciences and Technology, Physical Sciences, Chemistry – 03 P).

Evaluation Board:

Chairman – Prof. Habil. Dr. Albertas Malinauskas (Center for Physical Sciences and Technology, Physical Sciences, Chemistry – 03 P).

Members:

Prof. Dr. Ingrida Ancutienė (Kaunas University of Technology, Physical Sciences, Chemistry – 03 P),

Prof. Habil. Dr. Audrius Padarauskas (Vilnius University, Physical Sciences, Chemistry - 03 P),

Dr. Germanas Peleckis (Australian Wollongong University, Physical Sciences, Chemistry – 03 P),

Prof. Habil. Dr. Rimantas Ramanauskas (Center for Physical Sciences and Technology, Physical Sciences, Chemistry – 03 P).

The official discussion will be held at 2 p.m. on the 7th of July, 2017 at a public meeting of the Evaluation Board at the Auditorium of National Center for Physical Sciences and Technology.

Address: Saulėtekio ave. 3, LT – 10257 Vilnius, Lithuania.

The summary of doctoral dissertation was mailed on the 5th of June 2017.

The dissertation is available at the Library of Vilnius University, Library of Center for Physical Sciences and Technology and online: *www.vu.lt/lt/naujienos/ivykiu-kalendorius*.

VILNIAUS UNIVERSITETAS

FIZINIŲ IR TECHNOLOGIJOS MOKSLŲ CENTRAS

ALDONA BALČIŪNAITĖ

NAUJOS MEDŽIAGOS ŠARMINIAMS KURO ELEMENTAMS: SINTEZĖ, CHARAKTERIZAVIMAS IR SAVYBĖS

Daktaro disertacijos santrauka

Fiziniai mokslai, Chemija (03 P)

Vilnius 2017

Disertacija parengta 2012-2016 metais Fizinių ir technologijos mokslų centre Katalizės skyriuje.

Mokslinė vadovė – dr. Loreta Tamašauskaitė-Tamašiūnaitė (Fizinių ir technologijos mokslų centras, fiziniai mokslai, chemija – 03 P).

Disertacija ginama viešame Gynimo tarybos posėdyje:

Pirmininkas – prof. habil. dr. Albertas Malinauskas (Fizinių ir technologijos mokslų centras, fiziniai mokslai, chemija - 03 P).

Nariai:

prof. dr. Ingrida Ancutienė (Kauno technologijos universitetas, fiziniai mokslai, chemija - 03 P),

prof. habil. dr. Audrius Padarauskas (Vilniaus universitetas, fiziniai mokslai, chemija - 03 P),

dr. Germanas Peleckis (Australijos Volongongo universitetas, fiziniai mokslai, chemija - 03 P),

prof. habil. dr. Rimantas Ramanauskas (Fizinių ir technologijos mokslų centras, fiziniai mokslai, chemija - 03 P).

Disertacija bus ginama viešame Gynimo tarybos posėdyje 2017 m. liepos 7 d. 14 val. Nacionalinio fizinių ir technologijos mokslų centro salėje.

Adresas: Saulėtekio al. 3, LT – 10257 Vilnius, Lietuva.

Disertacijos santrauka išsiuntinėta 2017 m. birželio mėn. 5 d.

Disertaciją galima peržiūrėti Fizinių ir technologijos mokslų centro ir Vilniaus universiteto bibliotekose, bei VU interneto svetainėje adresu: *www.vu.lt/lt/naujienos/ivykiu-kalendorius*

1. INTRODUCTION

The thesis is related to the search of new effective materials, that can be used for development and design of direct borohydride fuel cells (DBFCs) in order to improve the performance of existing fuel cells or create novel fuel cells with high efficiency. The fuel cell is a device that converts the chemical reaction energy (e.g., oxidation of fuel) directly into electricity. Fuel cells are well-known as the cleanest method for energy production, because water is formed as a by-product, which does not pollute the environment.

The AuM (M = Ni, Co, Cu) catalysts deposited on the titanium (Ti) or titania nanotube arrayed (TiO_2-NTs) surfaces were fabricated by means of simple and low-cost electrochemical, electroless metal deposition and galvanic displacement techniques. The created catalysts are novel and and promising materials that can be used as anodes in direct borohydride fuel cells.

Development of renewable energy resources is important in order to reduce dependence on imported fuel. The rapid development of renewable energy sources and the capability of local energy generation has been growing in Lithuania in recent years.

The aim of the work was

Fabrication of efficient catalysts, their characterization and application for direct borohydride fuel cells.

The main tasks of the work were as follows:

1. Preparation of the Au(M)/Ti and Au(M)/TiO_2-NTs (M=Ni, Cu, Co) catalysts using the electroless metal deposition and galvanic displacement techniques.

2. Characterization of the surface morphology, structure and composition of the Au(M)/Ti and Au(M)/TiO_2-NTs catalysts by means of field emission scanning electron microscopy (FESEM), X-ray diffraction (XRD) and inductively coupled plasma optical emission spectroscopy (ICP-OES).

3. Determination of electrocatalytic properties of the Au(M)/Ti and Au(M)/TiO_2-NTs catalysts towards the electrooxidation of sodium borohydride using electrochemical methods.

Defensive statements:

1. Efficient AuM (M = Ni, Cu, Co) catalysts can be deposited on the Ti and TiO_2-NTs surfaces by means of the electroless metal deposition and galvanic displacement techniques.

2. The prepared Au(M)/Ti and Au(M)/TiO_2nv (M = Ni, Cu, Co) catalysts are electrocatalytically active with respect to the electrooxidation of sodium borohydride and are suitable for applying them as the anodes in direct borohydride fuel cells.

3. The Au(M)/Ti and Au(M)/TiO_2-NTs (M = Ni, Cu, Co) catalysts exhibit a significantly higher electrocatalytic activity towards the electrooxidation of sodium borohydride as compared with that of pure Au, M/Ti or M/TiO_2-NTs catalysts.

Novelty and actuality of the work

This thesis is related to the intensively developing research in the field of fuel cells and nanomaterials. The methodology for fabrication of the Au(M)/Ti and Au(M)/TiO_2-NTs (M = Ni, Cu, Co) catalysts with low Au loadings has been established. This methodology establishes sound scientific bases for developing efficient Au(M)/Ti and Au(M)/TiO_2-NTs catalysts with a significantly higher electrocatalytic activity towards the electrooxidation of sodium borohydride as compared to that of pure Au, M/Ti and M/TiO_2-NTs electrodes.

The novel catalysts, not used earlier, have been proposed for the oxidation of sodium borohydride. The highest electrocatalytic activity with respect to the electrooxidation of sodium borohydride has been obtained on the Au(Co)/Ti catalysts.

The prepared catalysts were applied as anode materials in the direct alkaline $NaBH_4$-H_2O_2 single fuel cell. These catalysts exhibit higher performance than the previously used catalysts in direct borohydride fuel cells. It has been found that these Au(M)/Ti and Au(M)/TiO_2-NTs catalysts can be successfully used in practical fuel cells as anodes.

2. EXPERIMENTAL

Chemicals. Titanium foil (99.7% purity, 0.127 mm thick), H_2SO_4 (95%), NH_4F (98%), $PdCl_2$ (59.5% Pd), C_2H_5OH (96%), $NiSO_4 \cdot 6H_2O$ (99%), $C_2H_5O_2N$ (99%), $NaH_2PO_2 \cdot H_2O$ (97%), $Na_2C_3H_2O_4$ (98%), $CuCl_2 \cdot 2H_2O$ (99%), $CoCl_2 \cdot 6H_2O$ (98%), $C_4H_{13}N_3$ (99%), $CoSO_4 \cdot 7H_2O$, (99.5%), $C_4H_{12}BNO$ (97%), $HAuCl_4 \cdot 3H_2O$ (99.9% Au), HCl (35-38%), $NaBH_4$ (96%) and NaOH (98.8%) were purchased from Sigma-Aldrich Supply. All chemicals were of analytical grade. Deionized (Elix 3 Millipore) water was used to prepare the electrolyte solutions. A Nafion N117 membrane was purchased from DuPont (Wilmington, DE).

Fabrication of catalysts. The self-ordered titania nanotube arrays (TiO_2-NTs) were prepared by anodic oxidation of Ti foil surface. Briefly, prior to anodization, titanium sheets (1 cm × 1 cm) were degreased with ethanol, rinsed with deionized water and dried in an Ar stream. Anodization of Ti sheets was performed in a 0.24 M H_2SO_4 solution with 0.5 wt.% NH_4F at a constant potential of 20 V at room temperature for 1 h. Two sheets of Pt were used as counter electrodes.

The M/Ti and M/TiO_2-NTs catalysts were prepared according to the following procedures: (i) activation of the Ti or TiO_2-NTs electrodes in a 1.7 mM $PdCl_2$ acidic solution for 60 s; (ii) subsequent rinsing of the activated surfaces with deionized water; (iii) followed by the immersion of the activated samples into the electroless Ni, Co or Cu plating baths. The Ni plating bath consists of 0.1 M $NiSO_4$, 0.4 M $C_2H_5O_2N$, 0.25 M NaH_2PO_2 and 0.1 M $C_3H_2O_4Na_2$. The bath operated at pH 9 and at a temperature of 85 ºC for 1 min.

The Co plating bath consisted of 0.05 M $NiSO_4$, 0.015 M diethylenetriamine and 0.05 M borane morpholine complex. The bath operated at pH 7 and at a temperature of 25 ºC for 45 min.

The Cu plating bath consisted of 0.05 M $CuCl_2$, 0.15 M $CoCl_2$ and 0.6 M diethylenetriamine. The bath operated at pH 6 and at a temperature of 20 ºC for 10 min.

The electroless Co and Cu plating baths were purged with Ar to remove air oxygen.

The Au crystallites were deposited on the prepared M/Ti or M/TiO_2-NTs electrodes by their immersion into 1 mM $HAuCl_4$ + 0.1 M HCl (denoted as Au(III)-containing solution) for 0.5, 1 and 5 min.

Characterization of catalysts. The surface morphology and composition of the fabricated catalysts were characterized using a SEM/FIB workstation Helios Nanolab 650 with an energy dispersive X-ray (EDX) spectrometer INCA Energy 350 X-Max 20.

The Au metal loading in the prepared catalysts was estimated using an ICP optical emission spectrometer Optima 7000DV (Perkin Elmer) at wavelengths of λ = 267.595 and 242.795 nm. For calibration, the standard solutions of 1.0 and 10.0 mg l^{-1} were used (Perkin Elmer).

XRD patterns of the prepared catalysts were measured using an X-ray diffractometer SmartLab (Rigaku) equipped with an 9 kW X-ray tube with a rotating Cu anode. The grazing incidence (GIXRD) method was used in the 2Θ range 35 – 80°. The angle between the parallel beam of X-rays and a specimen surface (ω angle) was adjusted to 0.5°.

Electrochemical measurements. Electrochemical measurements were performed with a Metrohm Autolab potentiostat (PGSTAT100) using a conventional three-electrode electrochemical cell. The M/Ti, M/TiO_2-NTs, Au(M)/Ti and Au(M)/TiO_2-NTs catalysts with a geometric area of 2 cm^2 were employed as working electrodes, an Ag/AgCl/KCl_{sat} electrode was used as reference and a Pt sheet was used as a counter electrode. An Au-sputtered quartz crystal with a geometric area of 0.636 cm^2 was used as a bare Au electrode.

The electrochemically active areas of Au surface (ESAs) in the catalysts were determined from the cyclic voltammograms of bare Au, Au(M)/Ti and Au(M)/TiO_2-NTs catalysts recorded in a deaerated 0.5 M H_2SO_4 solution at a scan rate of 50 mV s^{-1}. The ESAs of Au nanoparticles in the catalysts were calculated by the charge associated with the Au surface oxide reduction peak (400 μC cm^{-2} for a monolayer) [3].

Sodium borohydride oxidation was investigated by recording cyclic voltammograms (CVs) in a 1 M NaOH solution containing 0.05 M $NaBH_4$ at a potential scan rate of 10 mV s^{-1} from the open circuit potential values in the anodic direction up to 0.6 V vs. Ag/AgCl/KCl_{sat} at a temperature of 25 ºC. The chronoamperometric curves for the M/Ti,

M/TiO_2-NTs, Au(M)/Ti and Au(M)/TiO_2-NTs catalysts were recorded at a constant potential values for 2 min.

Fuel cell test experiments. Direct borohydride-hydrogen peroxide fuel cell (DBHPFC) tests were carried out by employing the M/Ti, M/TiO_2-NTs, Au(M)/Ti and Au(M)/TiO_2-NTs catalysts (with a geometric area of 2 cm^2) as the anode and a Pt sheet with a geometric area of 6 cm^2 as the cathode. Each compartment of the cell contained 100 mL of the corresponding aqueous electrolyte. The anolyte was composed of an alkaline mixture of 1 M $NaBH_4$ + 4 M NaOH and the catholyte containing 5 M H_2O_2 + 1.5 M HCl. To prevent H_2O_2 decomposition and possible loss of BH_4^- by hydrolysis during storage, the test solutions were prepared immediately before the measurements. A Nafion® N117membrane was used to separate the anodic and cathodic compartments of the single direct $NaBH_4$-H_2O_2 fuel cell. The active area of membrane was ca. 30 cm^2. Cell measurements were conducted using a Zennium electrochemical workstation (ZAHNER-Elektrik GmbH & Co. KG). The performance of the fuel cell was evaluated by recording the cell polarization and obtaining the corresponding power density curves.

3. RESULTS AND DISCUSSIONS

3.1 Characterization of catalysts

The Au(M)/Ti and Au(M)/TiO_2-NTs (M = Ni, Co, Cu) catalysts were prepared by partial galvanic displacement of electroless metal layers, deposited on the Ti and TiO_2-NTs surfaces, by Au nanoparticles from the Au(III)-containing solution.

Self-ordered TiO_2 nanotube arrays in this study were prepared by anodic oxidation of Ti surface in an aqueous sulfuric acid solution containing NH_4F. The average tube diameter was ca. 100 nm and the thickness of titania nanotubes was ~310 nm (Fig. 1).

The electroless Ni layer with the thickness of ca. 300 nm was deposited on the titanium and titania nanotube surfaces, which produces a layer of granular nickel crystallites ca. 200 nm in size (Fig. 2 a,b). The data of EDX analysis are given in Table I. It should be noted that the nickel layer is deposited on the Ti or TiO_2-NTs surfaces in the electroless

plating solution using sodium hyphophosphite as a reducing agent. So, about 9 at.% of phosphorus is co-deposited with Ni.

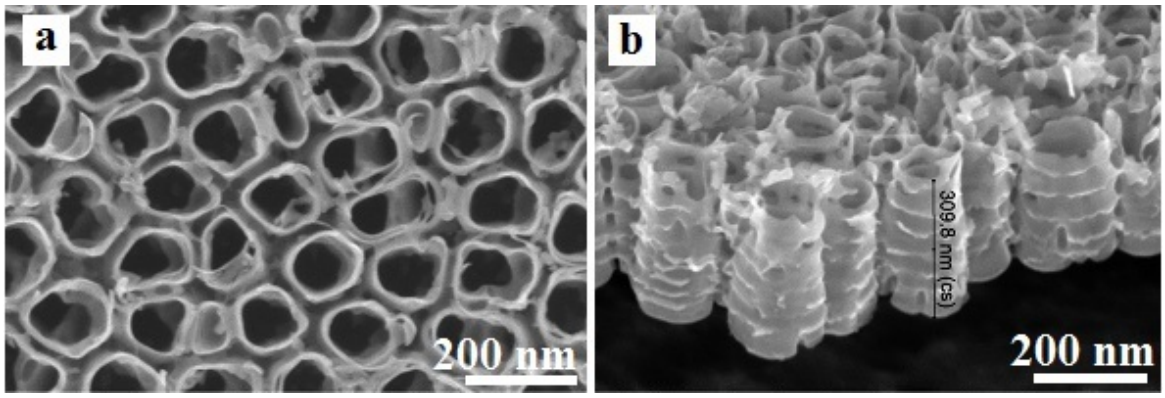

Fig. 1. SEM micrographs of top side (a) and cross-sectional side view (b) of as-prepared TiO_2-NTs.

TABLE I. The contents of elements on the surface of the Ni/Ti and Ni/TiO_2-NTs electrodes by EDX analysis. The catalysts are the same as in Figure 2 (a,b).

Catalysts	Elements, at.%				Size of crystallites, μm
	Ni	P	O	Ti	
Ni/Ti	62.73	9.39	8.13	19.93	0.2
Ni/TiO_2-NTs	79.65	8.40	2.96	8.99	0.2

The layers of polycrystalline Co with average crystallites size of ca. 400-900 nm and 400-1000 nm and the thickness of ca. 1.1 μm were deposited on the Ti and TiO_2-NTs surfaces, respectively (Fig. 2 c,d). The data of EDX analysis are shown in Table II.

TABLE II. The contents of elements on the surface of the Co/Ti and Co/TiO_2-NTs catalysts by EDX analysis. The catalysts are the same as in Figure 2(c,d).

Catalysts	Elements, at.%			Size of crystallites, μm
	Co	O	Ti	
Co/Ti	34.82	24.41	40.78	0.4-0.9
Co/TiO_2-NTs	66.16	21.17	12.67	0.4-1

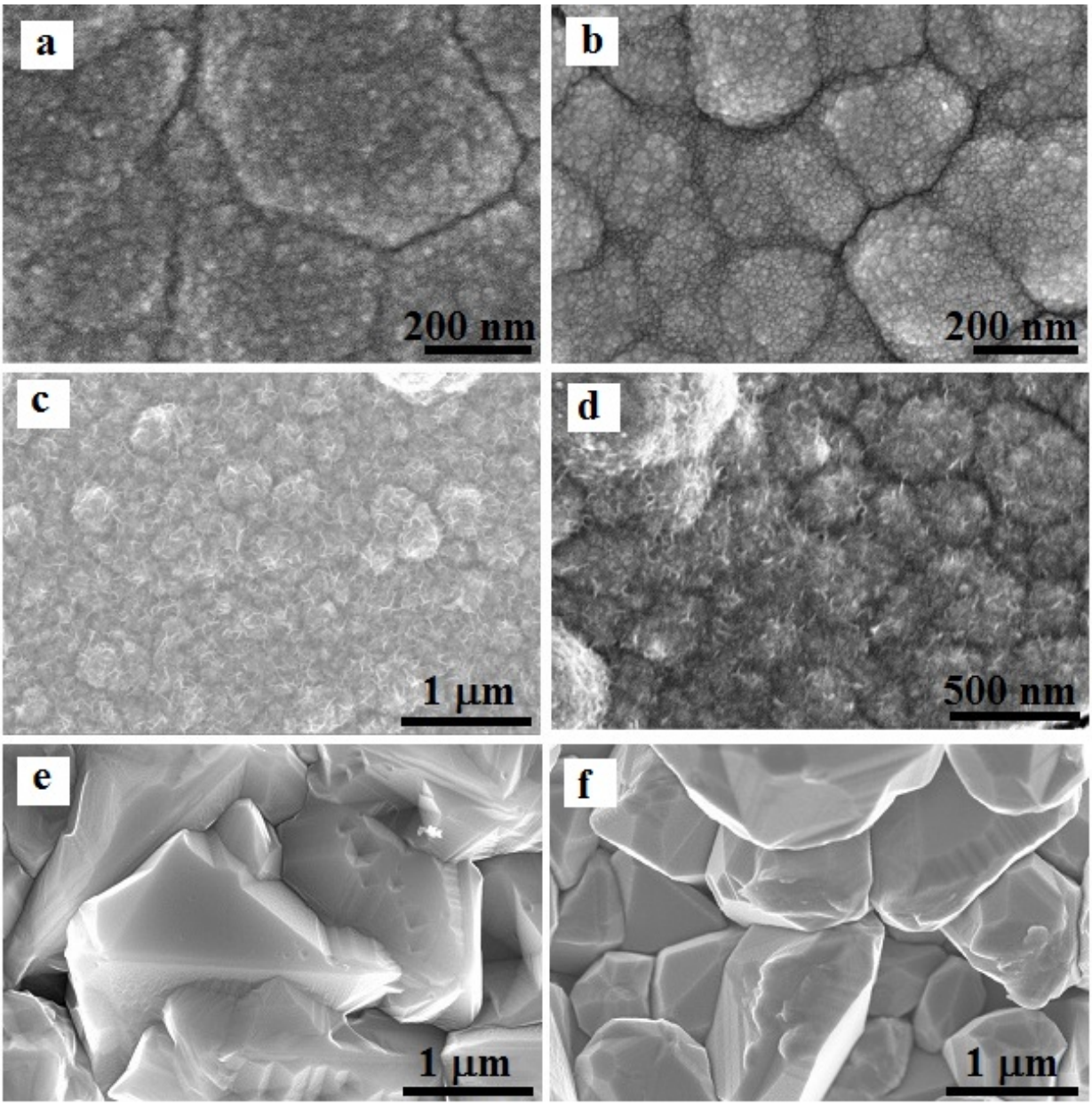

Fig. 2. SEM micrographs of the top side views of as-prepared Ni/Ti (a), Ni/TiO_2-NTs (b) Co/Ti (c), Co/TiO_2-NTs (d), Cu/Ti (e) and Cu/TiO_2-NTs (f). The M/Ti and M/TiO_2-NTs catalysts were prepared by immersion of Ti or TiO_2-NTs into the Ni plating bath at 85 ºC for 1 min (a,b), Co plating bath at 25 ºC for 45 min (c,d) and Cu plating bath at 20 ºC for 10 min (e,f).

The layers of polycrystalline Cu with the average size of crystallites of ca. 1 μm and the thickness of ca. 1.5 μm were deposited on the Ti and TiO_2-NTs surfaces (Fig. 2 e,f). The data of EDX analysis of the as-prepared catalysts are given in Table III.

TABLE III. The contents of elements on the surface of the Cu/Ti and Cu/TiO_2-NTs catalysts by EDX analysis. The catalysts are the same as in Figure 2 (e,f).

Catalysts	Elements, at.%			Size of crystallites, μm
	Cu	O	Ti	
Cu/Ti	97.74	1.24	1.02	1
Cu/TiO_2-NTs	94.93	2.33	2.74	1

The Au nanoparticles were deposited on the M/Ti or M/TiO_2-NTs surfaces by galvanic displacement. Immersion of the M/Ti or M/TiO_2-NTs surfaces into 1 mM $HAuCl_4$ + 0.1 M HCl for 0.5, 1 and 5 min results in deposition of Au crystallites on the surface of M/Ti or M/TiO_2-NTs. The SEM views of prepared Au(M)/Ti and Au(M)/TiO_2-NTs catalysts are presented in Figs. 3-5. The Au nanoparticles of ca. 10-50 nm and 10-30 nm in size were deposited on the Ni/Ti (Fig. 3a-c) and Ni/TiO_2-NTs (Fig. 3d-f) electrodes, respectively, after their immersion into the Au(III)-containing solution for 0.5, 1 and 5 min (Fig. 3). The Au crystallites appear as bright spots and they are quite uniform in size and well separated (Fig. 3).

As evident from Fig. 4, the Au crystallites of the cubic shape and homogeneously dispersed were deposited on the Co/Ti (Fig. 4a-c) and Co/TiO_2-NTs (Fig. 4d-f). After immersion of the Co/Ti and Co/TiO_2-NTs electrodes into the Au(III)-containing solution for 0.5, 1 and 5 min, the Au crystallites of ca. 15-100 nm and 10-75 nm in size were deposited on Co/Ti (Fig. 4a-c) and Co/TiO_2-NTs (Fig. 4d-f), respectively.

Immersion of the Cu/Ti and Cu/TiO_2-NTs electrodes in an Au(III)-containing solution for 0.5, 1 and 5 min, respectively, results in deposition of Au nanoparticles sized 10 to 50 nm (Fig. 5).

The summarized data of investigated Au(M)/Ti and Au(M)/TiO_2-NTs catalysts by EDX analysis are given in Table IV. The analysis of all prepared Au(M)/Ti and Au(M)/TiO_2-NTs catalysts confirms the presence of Au , Ni, Co and Cu on the Ti and TiO_2-NTs electrodes. In all cases, significant amounts of deposited Ni, Co or Cu and a much lower amount of Au were detected on the surface of catalysts (Table IV).

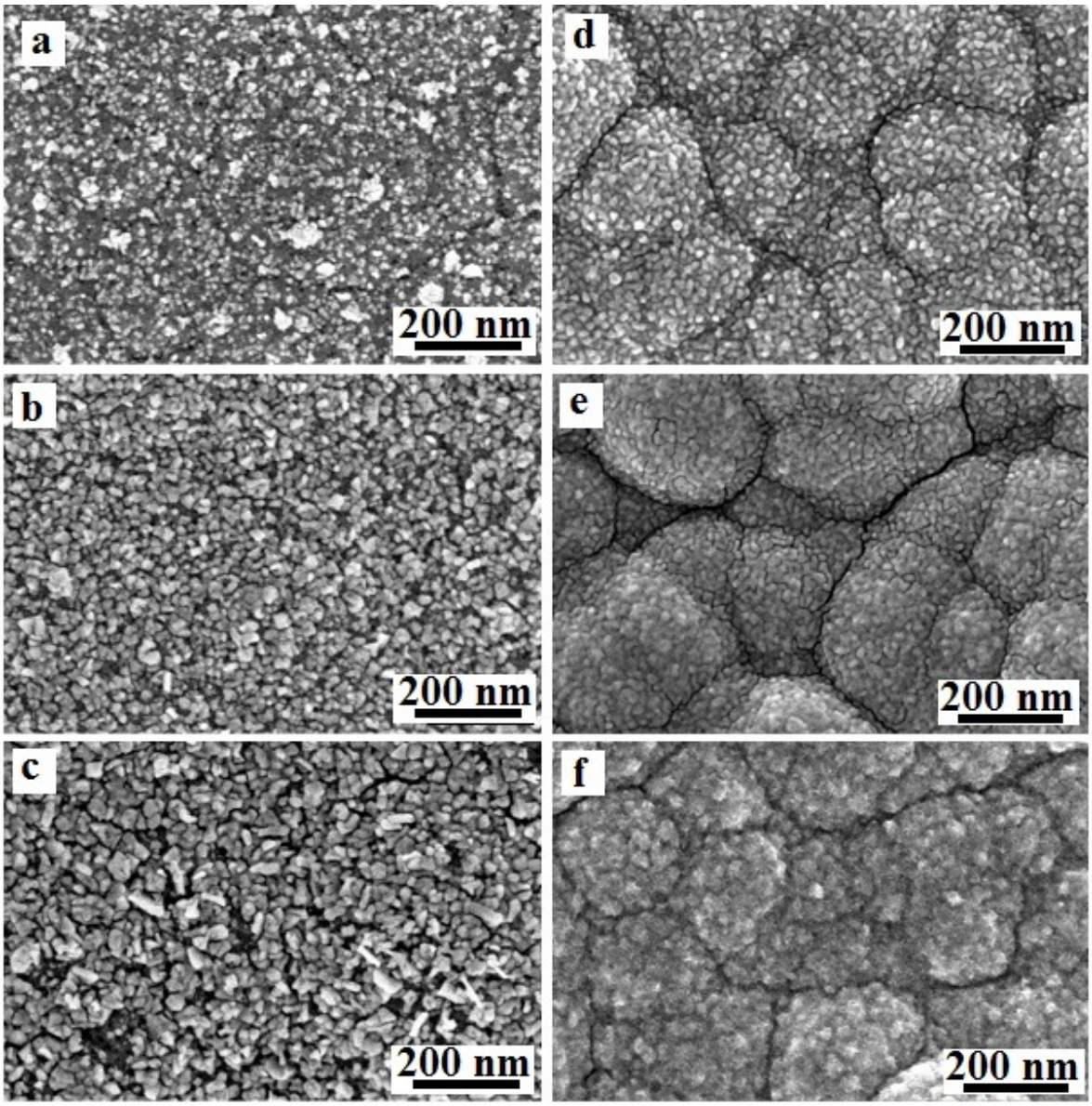

Fig. 3. SEM micrographs of top side views of as-prepared Au(Ni)/Ti (a-c) and Au(Ni)/TiO_2-NTs (d-f) catalysts. The catalysts were prepared by immersion of Ti or TiO_2-NTs into the Ni plating bath at 85 ºC for 1 min, followed by their immersion in 1 mM $HAuCl_4$ + 0.1 M HCl at 25 ºC for 0.5 (a,d), 1 (b,e) and 5 (c,f) min.

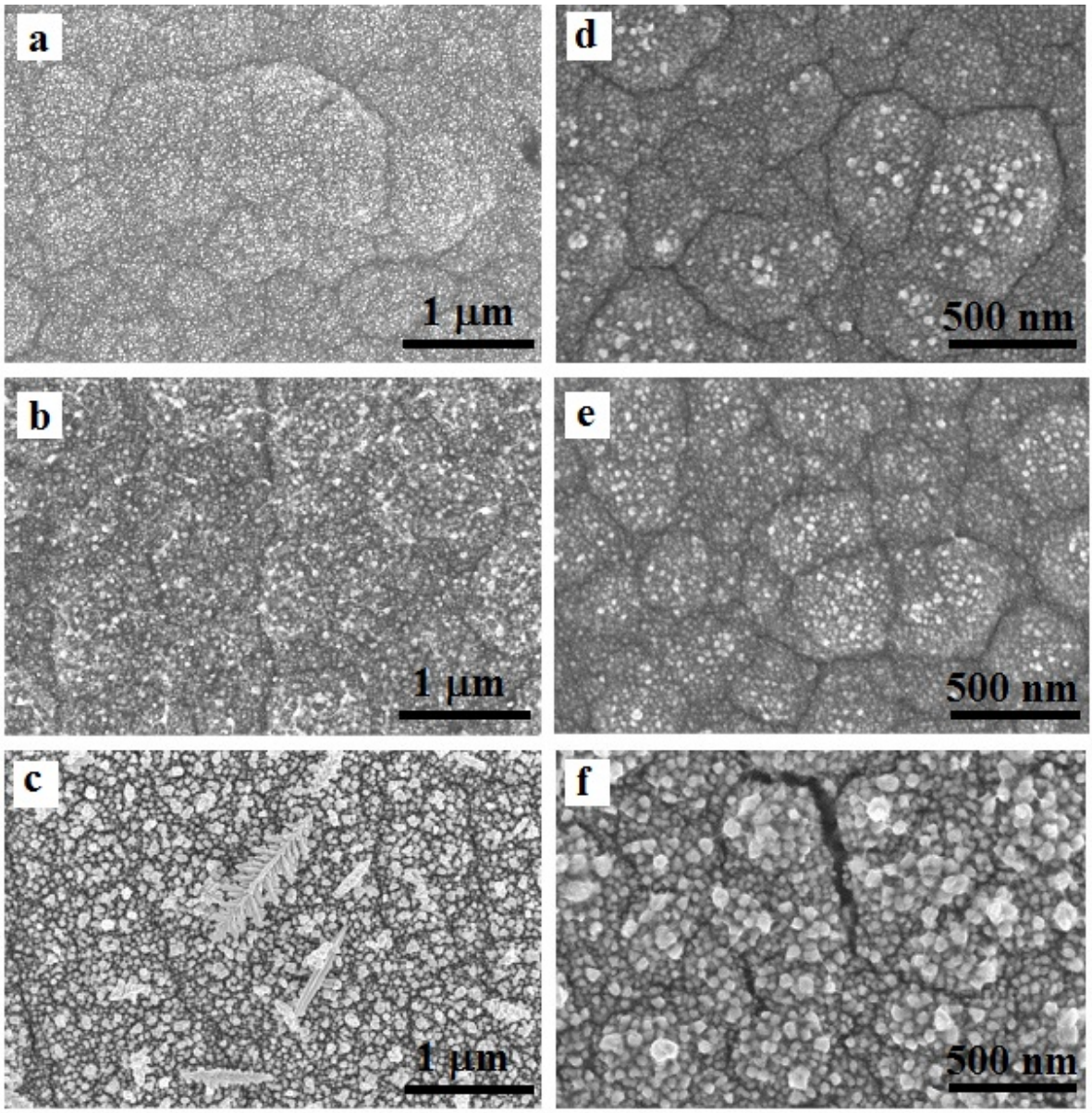

Fig. 4. SEM micrographs of top side views of as-prepared Au(Co)/Ti (a-c) and Au(Co)/TiO_2-NTs (d-f) catalysts. The catalysts were prepared by immersion of Ti or TiO_2-NTs into the Co plating bath at 25 ºC for 45 min, followed by their immersion in 1 mM $HAuCl_4$ + 0.1 M HCl at 25 ºC for 0.5 (a,d), 1 (b,e) and 5 (c,f) min.

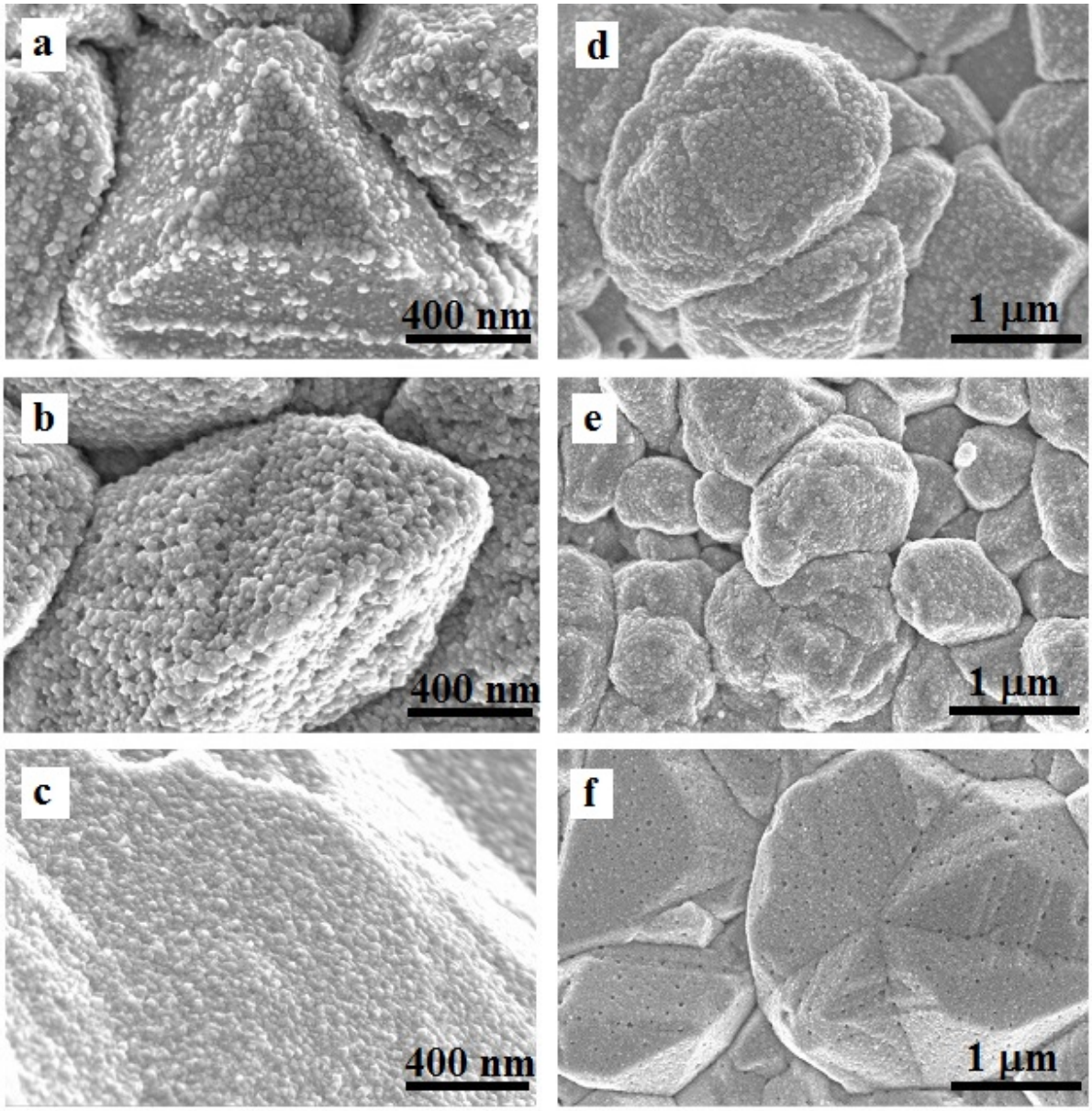

Fig. 5. SEM micrographs of top side views of as-prepared Au(Cu)/Ti (a-c) and Au(Cu)/TiO_2-NTs (d-f) catalysts. The catalysts were prepared by immersion of Ti or TiO_2-NTs into the Cu plating bath at 20 ºC for 10 min, followed by their immersion in 1 mM $HAuCl_4$ + 0.1 M HCl at 25 ºC for 0.5 (a,d), 1 (b,e) and 5 (c,f) min.

TABLE IV. The contents of elements on the surface of the Au(M)/Ti and Au(M)/TiO_2-NTs catalysts by EDX analysis. The catalysts are the same as in Figures 3, 4 and 5. The Au loadings were estimated from ICP-OES measurements.

Au(Ni)/Ti and Au(Ni)/TiO_2-NTs catalysts

Catalysts	Au deposition time, min	Elements, at.%					Particle size, nm	Au loading, μg cm^{-2}	ESA, cm^2
		Au	Ni	P	O	Ti			
Au(Ni)/Ti	0.5	0.23	51.47	7.46	2.69	38.14	10-30	0.9	3.3
	1	0.61	53.18	7.25	2.36	36.60	10-30	1.8	5.5
	5	1.29	46.00	5.12	4.64	42.95	10-50	8.4	6.6
Au(Ni)/TiO_2-NTs	0.5	0.34	73.86	5.18	3.22	17.41	10-30	8.2	1.3
	1	0.62	74.54	5.47	3.27	16.10	10-30	10.6	2.7
	5	1.38	71.56	5.65	3.98	17.44	10-30	34.1	4.2

Au(Co)/Ti and Au(Co)/TiO_2-NTs catalysts

Catalysts	Au deposition time, min	Elements, at.%				Particle size, nm	Au loading, μg cm^{-2}	ESA, cm^2
		Au	Co	O	Ti			
Au(Co)/Ti	0.5	0.22	54.60	31.86	13.32	15-50	4.2	0.7
	1	1.01	58.61	27.81	12.58	15-50	16.9	2.0
	5	2.86	27.80	48.34	21.01	30-100	57.6	6.9
Au(Co)/TiO_2-NTs	0.5	0.35	38.83	41.21	19.61	10-35	10.0	1.4
	1	0.51	32.50	49.55	17.44	10-40	22.2	2.2
	5	1.16	14.89	61.27	22.68	10-75	59.4	3.8

Au(Cu)/Ti and Au(Cu)/TiO_2-NTs catalysts

Catalysts	Au deposition time, min	Elements, at.%				Particle size, nm	Au loading, μg cm^{-2}	ESA, cm^2
		Au	Cu	O	Ti			
Au(Cu)/Ti	0.5	1.77	95.49	1.04	1.71	10-50	5.6	1.1
	1	2.73	94.67	1.27	1.34	10-50	9.8	3.9
	5	6.87	91.14	0.75	1.24	10-50	19.8	7.9
Au(Cu)/TiO_2-NTs	0.5	0.29	91.29	6.21	2.21	10-50	8.5	1.7
	1	0.46	88.03	6.39	5.13	10-50	11.3	2.2
	5	1.35	92.65	4.64	1.36	10-50	23.4	7.5

The Au metal loadings in the Au(M)/Ti and Au(M)/TiO_2-NTs catalysts were determined by means of inductively coupled plasma optical emission spectroscopy and are given in Table IV. It has been determined that the Au loadings were 0.9, 1.8 and 8.4 $\mu g_{Au}\, cm^{-2}$ and 8.2, 10.6 and 34.1 $\mu g_{Au}\, cm^{-2}$ in the fabricated Au(Ni)/Ti and Ni/TiO_2-NTs, respectively, catalysts after sonication of the Ni/Ti and Ni/TiO_2-NTs electrodes in an Au(III)-containing solution for 0.5, 1 and 5 min, respectively.

After immersion of the Co/Ti and Co/TiO_2-NTs electrodes into the Au(III)-containing solution for 0.5, 1 and 5 min, the Au nanoparticles with the Au loadings of 4.2, 16.9, 57.6 $\mu g_{Au} cm^{-2}$ and 10, 22, 59 $\mu g_{Au} cm^{-2}$, respectively, were deposited on Co/Ti and Co/TiO_2-NTs.

Then the Cu/Ti and Cu/TiO_2-NTs electrodes were immersed in an Au(III)-containing solution for 0.5, 1 and 5 min, respectively, the Au(Cu)/Ti and Au(Cu)/TiO_2-NTs catalysts were prepared with the Au loadings of 5.6, 9.8, 19.8 $\mu g_{Au}\, cm^{-2}$ and 8.5, 11.3, 23.4 $\mu g_{Au}\, cm^{-2}$, respectively (Table IV).

The electrochemically active areas of the surface of Au nanoparticles (ESA) in the catalysts were determined from the cyclic voltammograms of the Au, Au(M)/Ti and Au(M)/TiO_2-NTs catalysts recorded in a deaerated 0.5 M H_2SO_4 solution at a scan rate of 50 mV s^{-1} by calculating the charge associated with Au oxide reduction (400 $\mu C\, cm^{-2}$ for a monolayer). The data obtained are given in Table IV. It should be noted that the ESA of pure Au electrode was 1.6 cm^2. The results show that the ESAs values of the catalysts prepared by immersion of M/Ti and M/TiO_2-NTs in an Au(III)-containing solution for 1 and 5 min, respectively, are ca. 2-5 times higher than those of pure Au.

Figure 6 a shows XRD patterns for the Ni/TiO_2-NTs (lower black colour pattern) and Au(Ni)/TiO_2-NTs catalysts prepared by immersion of Ni/TiO_2-NTs in a 1 mM $HAuCl_4$ + 0.1 M HCl solution at 25 ^oC for 1 and 5 min (upper curves). The presented 2Θ ranges contain sharp XRD peaks of the Ti substrate and broad ones of Ni 111, Au 111, Au 200 and Au 220 (in the inset). The XRD peak Au 111 overlaps with that of Ti 002 and peak Au 200 with that of Ni 111. The presence of the Au can be apparently evidenced by the inset of Fig. 6 a.

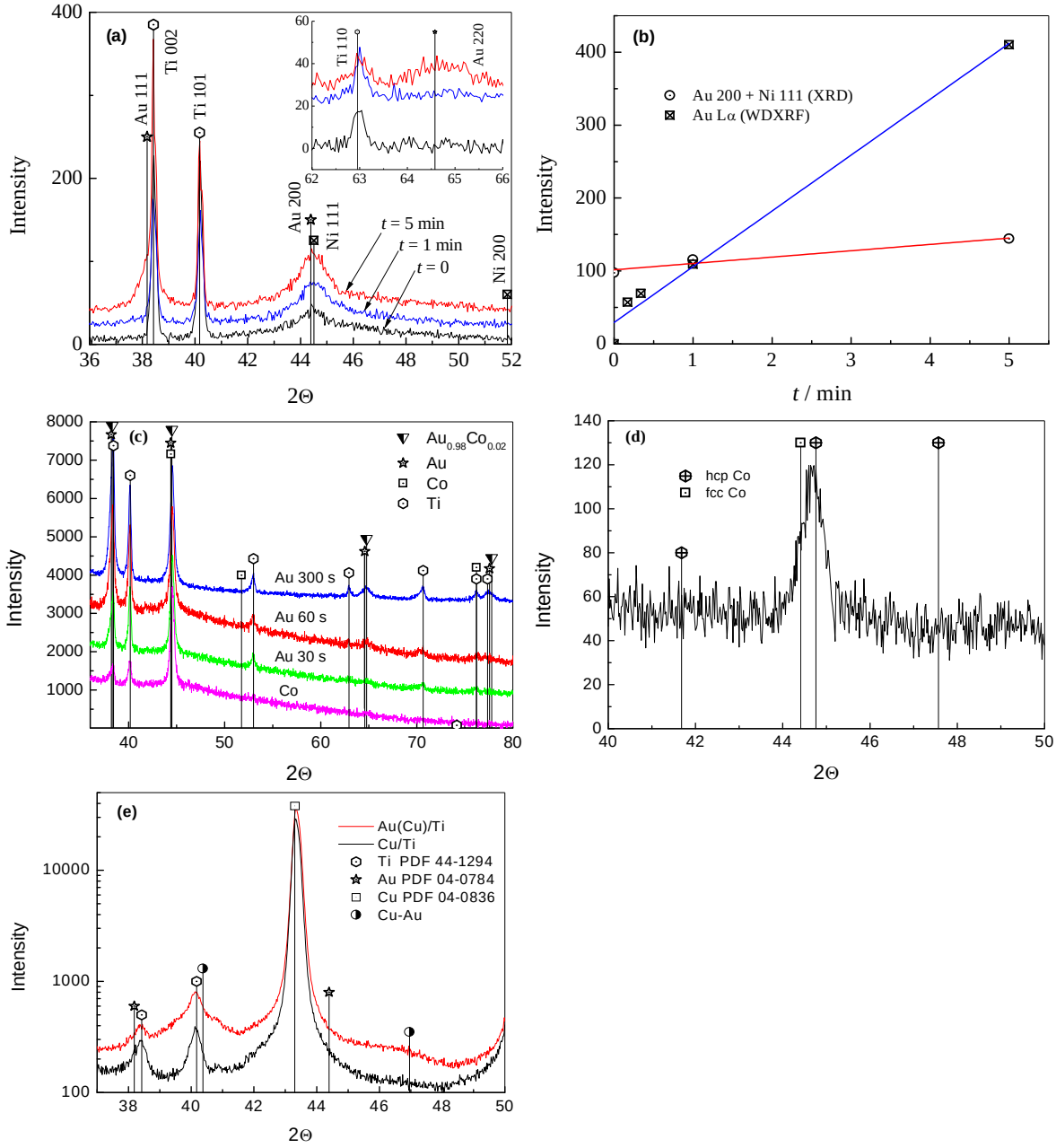

Fig. 6. XRD patterns: (a) Ni/TiO_2-NTs (lower black colour pattern) and Au(Ni)/TiO_2-NTs prepared by immersion of Ni/TiO_2-NTs in 1 mM $HAuCl_4$ + 0.1 M HCl at 25 °C for 1 and 5 min (upper curves); (b) The integral intensity of the overlapping XRD peaks Au 200 and Ni 111 and intensity Au Lα peak of the x-ray spectrum for Au layers with different deposition time; (c) Co/Ti and Au(Co)/Ti, the same as in Fig. 4 (a-c); (d) Co layer measured using the in-plane technique; (e) Cu/Ti (upper curve) and Au(Cu)/Ti prepared by immersion of Ti sheets in the Cu plating bath at 20 °C for 10 min, followed by its immersion in 1 mM $HAuCl_4$ + 0.1 M HCl at room temperature for 5 min.

The upper curve corresponding to Au(Ni)/TiO_2-NTs, when duration of Au deposition was 5 min (t_{Audep} = 5 min), shows a broad peak at the position of XRD peak Au 220 according to PDF No 04-0784. There is no peak at this position in the lower XRD patterns corresponding to Au(Ni)/TiO_2-NTs (t_{Audep} = 1 min) and Ni/TiO_2-NTs (t_{Audep} = 0 min), respectively. The presence of Au is also evidenced by a hump on the left shoulder of the XRD peak Ti 002 in the pattern (upper red curve) for the Au(Ni)/TiO_2-NTs (t_{Audep} = 5 min) catalyst. It was difficult to determine precisely the value of the lattice parameter of Au due to low intensity and broadening of the peaks, however, it may be suggested that the Au peaks were a little bit shifted towards higher diffraction angles. That points to the formation of Ni solid solution in gold. The presence of the Au layer can be supported by Fig. 6 b, which shows an integral intensity of the XRD peaks Au 200 and Ni 111 as a function of Au deposition time. Since the thickness of Ni layer was always the same, the increase in the integral intensity of the overlapping peaks Au 200 and Ni 111 must be related with the increase in thickness of Au layer. Fig. 6 b also presents results of WDXRF measurements, i.e. the intensity of the Au Lα peak of characteristic X-ray spectrum for the Au layers obtained at the Ni/TiO_2-NTs substrate at different deposition periods, which also supported the increase in thickness of the Au layer.

Figure 6 c shows XRD patterns for Co/Ti (lower curve) and Au(Co)/Ti prepared by immersion of Co/Ti in 1 mM $HAuCl_4$ + 0.1 M HCl for different periods (upper curves). The symbols indicate the positions of the XRD peaks of Ti (PDF card no 00-044-1294), Au (00-004-0784), Co (00-015-0806) and $Au_{0.98}Co_{0.02}$ (04-001-1901). The lowest XRD pattern contains three XRD peaks of Ti substrate and only one strong peak attributable to Co. To ascertain which crystalline structure presents the cobalt layer – cubic face centered (fcc) structure or hexagonal (hcp) one, the XRD in-plane measurement was conducted since that enables to measure XRD peaks from crystallographic planes perpendicular to the sample surface. Figure 6 d shows the obtained XRD pattern, which evidences that there are no XRD peaks of the hcp structure, which does not overlap with the peak of fcc Co 111. However, XRD peak Co 111 is slightly shifted towards higher diffraction angles. Since Co was deposited using morpholine borane as a reducing agent, some amount of boron (in our case

up to 1 %) could be intercalated into the cobalt deposit; therefore, the above-mentioned shift could be explained by formation of a replacement solid solution of boron in cobalt.

Figure 6 e presents XRD patterns for Cu/Ti and Au(Cu)/Ti prepared by immersion of Cu/Ti electrode in a 1 mM $HAuCl_4$ + 0.1 M HCl solution at 25 °C for 5 min (upper curve). The presented 2Θ ranges contain XRD peaks: 100 and 002 of the Ti substrate and a strong peak 111 of Cu in the case of Cu/Ti. When Au was deposited on the Cu layer, two broad additional peaks appeared at the diffractions angles of ~40 and ~47°. The maxima of the peaks corresponded to the positions of peaks 111 and 200 of an fcc crystalline structure with the lattice parameter of 0.3867 nm. It could be believed that these peaks are of fcc phase of a continuous solid solution of Au and Cu. According to the relationship of lattice parameters and composition in the disordered fcc phase in the Au-Cu system, the proportion of Au in the solid solution was determined and it approximately equalled to 45 at.%. The broad XRD peaks (FWHM = 1.25° for the peak with a maximum at 47°) of the solid solution pointed to a very thin layer of the Au-Cu phase. On the other hand, the broadening of the peaks could be also caused by the inhomogeneity of the composition of the Au-Cu solid solution.

3.2. Electrochemical characterization

The electrocatalytic activity of the prepared catalysts towards the oxidation of BH_4^- ions was evaluated by cyclic voltammetry. Fig. 7 shows the oxidation of BH_4^- ions on the bulk Au electrode in 1.0 M NaOH containing 0.05 M $NaBH_4$ at a temperature of 25◦C with a scan rate of 10 mV s^{-1}. Broad peaks of the direct oxidation of BH_4^- for bulk Au are observed at a potential of ca. -0.4 V (anodic peaks **A**), which is attributed to the direct oxidation of BH_4^- ions. Wide oxidation waves that extend up to 0.4 V correspond to the oxidation of reaction intermediates on the partially oxidized Au surface. In the backward scan, sharp peaks **B** are observed at ca. 0.2 V followed by a plateau in the potential region from 0 to -0.6 V. These peaks are attributed to the oxidation of the adsorbed species such as BH_3OH^- or other borohydrides formed as an intermediate during the oxidation of the BH_4^- ion in the forward scan.

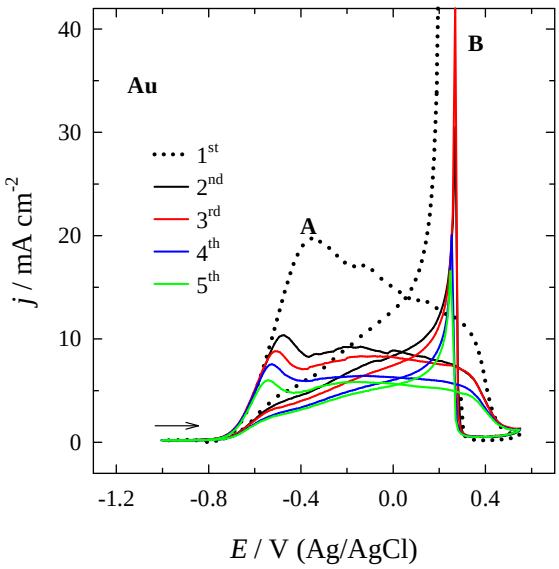

Fig. 7. CVs of bare Au in 0.05 M $NaBH_4$ + 1 M NaOH at 25 ºC with a sweep rate of 10 mV s^{-1}.

The oxidation of borohydride was investigated on the Ni/Ti, Co/Ti and Cu/Ti electrodes by cyclic voltammetry. Figure 8 a presents the CVs for Ni/Ti in 1.0 M NaOH (*the inset a'*) and in that containing 0.05 M $NaBH_4$ at 25 ºC with a scan rate of 10 mV s^{-1}.

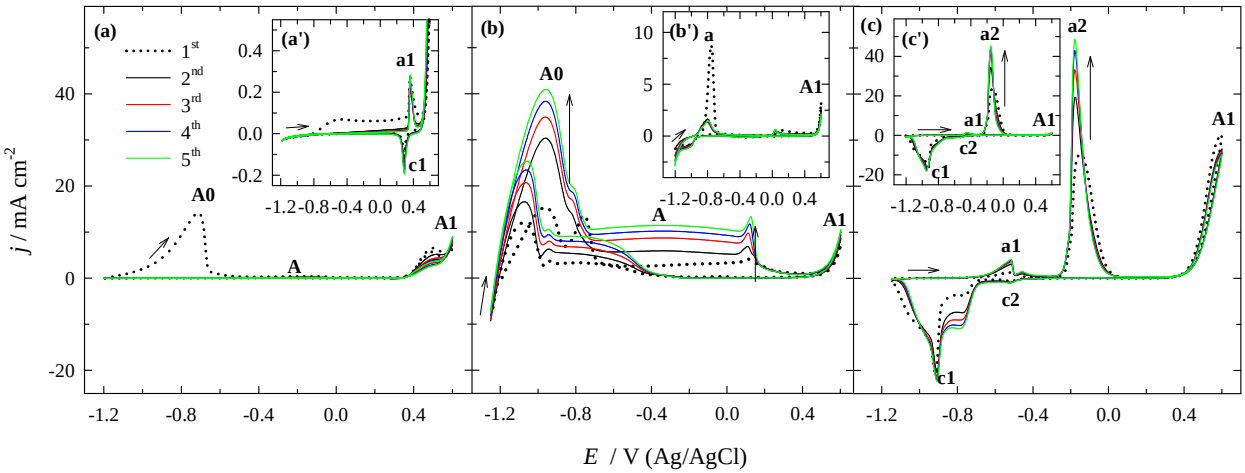

Fig. 8. Borohydride oxidation recorded on Ni/Ti (a), Co/Ti (b) and Cu/Ti (c) in 0.05 M $NaBH_4$ + 1 M NaOH at 10 mV s^{-1}; 25 ºC. The insets represent the CVs of Ni/Ti (a'), Co/Ti (b') and Cu/Ti (c') recorded in 1 M NaOH.

As seen from the inset in Fig. 8 a', during the forward sweep, well-defined anodic (**a1**) and cathodic (**c1**) peaks are recorded. The peaks are associated with the transformation between β-$Ni(OH)_2$ and β-NiOOH. The anodic and cathodic potentials were at ca. 0.36 and 0.29 V. An addition of 0.05 M $NaBH_4$ to the 1.0 M NaOH solution (Fig. 8 a) results in anodic peak **A0** at more negative potential values at ca. -0.8 V. According to the literature, this peak is attributed to the oxidation of H_2, generated by the catalytic hydrolysis of BH_4^-. At potentials higher than 0.4 V anodic peak **A1**, which corresponds to the oxidation reaction of $Ni(OH)_2 \rightarrow NiOOH$ is recorded, while the cathodic response of this reaction is not observed on the backward sweep. Hence, during the subsequent anodic scans no anodic peaks were observed at lower potential values. It may be proposed that the Ni layer deposited on the Ti surface does not catalyze the direct BH_4^- ions oxidation at higher potentials due to the passivation caused by nickel hydroxide(s) formation or, maybe, the surface of catalyst is poisoned by strongly adsorbed intermediates generated during the BH_4^- ion oxidation or sodium borohydride oxidation on the metal surface of Ni.

The borohydride oxidation on Co/Ti is shown in Figure 8 b. In the case of Co/Ti in 1 M NaOH (Fig. 8b, the inset b'), during anodic scan anodic peak **a** is observed at lower potential values. This anodic peak at ca. -0.8 V can be attributed to the formation of Co hydroxides/oxides in the alkaline medium at low potential values. The measured sodium borohydride oxidation current density values at Co/Ti are significantly greater as compared to those recorded in the background solution (1 M NaOH) at the latter catalyst (Fig. 8b). Two well-expressed anodic peaks **A0** and **A** are observed in the CVs recorded on the Co/Ti electrode in a 0.05 M $NaBH_4$ +1 M NaOH solution. The measured oxidation current densities under the low-potential region from -1.2 to -0.7 V (peak **A0)** recorded on Co/Ti may be ascribed to the direct oxidation of borohydride anion. Based on the ground of FTIR, EQCM and RDDE investigations of the overall borohydride oxidation process on various catalysts show that the mechanism of borohydride oxidation is rather complicated due to the formation of intermediates, adsorption phenomenon and influence of electrode potential, e.g., formation, adsorption and oxidation of BH_3OH^-. It may be assumed that in the low-potential region up to < -0.7 V borohydride oxidation on the Co/Ti electrode proceeds via

fully dissociative adsorption of BH_4^-. It was shown that in the low-potential region direct BH_4^- electrooxidation produces more electrons then the high-potential direct BH_4^- electro-oxidation. In the case when potential values are more positive than 0.4 V, anodic peak **A1** is observed. This peak may be attributed to the formation of Co(III) surface compounds.

The electrochemical behavior of Cu/Ti electrode in the 1 M NaOH solution (the inset c') and in that containing 0.05 M $NaBH_4$ at a sweep rate of 10 mV s^{-1} is shown in Fig. 8 (c). The CVs recorded for the Cu/Ti electrode in both solutions are similar in shape except those at potential values higher than 0.4 V. Anodic peak **a1** at a potential value of -0.5 V is attributed to the formation of insoluble Cu(I) compounds and anodic peak **a2** at -0.25 V – to the formation of insoluble Cu(II) compounds. Also during the backward scan, reduction peaks **c1** and **c2** are seen in the cathodic part. These peaks correspond to the reduction of the insoluble Cu(I) and Cu(II) compounds formed previously during the anodic scan (Fig. 8 c,c'). Anodic peaks **A1** observed at potentials higher than 0.5 V presumably correspond to the Cu(III)/Cu(II) couple which always appears in the course of the oxidation of copper in strongly alkaline solutions. The formal reduction potential of Cu(III)/Cu(II) in a 1 M NaOH solution stands at 0.56 V vs. Ag/AgCl. It should be mentioned that sodium borohydride is inactive at the Cu/Ti electrodes at low potentials. Enhanced anodic currents (peak **A1**) are observed under the potential region of Cu(II)/Cu(III) transition and may be related with the strong interaction of sodium borohydride with the surface already covered by insoluble Cu(II) compounds.

Figure 9 shows positive-going potential stabilized scans (5^{th} cycle) of the oxidation of BH_4^- ions recorded on bare Au, M/Ti, M/TiO_2-NTs, Au(M)/Ti and Au(M)/TiO_2-NTs catalysts with different Au loadings. The oxidation peaks observed at a potential of -0.8 V (peak **A0**) is attributed to the oxidation of H_2, generated by the catalytic hydrolysis of BH_4^-. The current density values are significantly higher in comparison with the current density values obtained using pure Au, Ni/Ti or Ni/TiO_2-NTs electrodes (Fig. 9 a,b). It proves that the prepared Au(Ni)/Ti and Au(Ni)/TiO_2-NTs catalysts have a higher catalytic activity for direct sodium borohydride oxidation. The direct oxidation peak current densities of BH_4^- (peak **A)** for the Au(Ni)/Ti and Au(Ni)/TiO_2-NTs (Fig. 9 a,b) catalysts with different Au

loadings are ca. 10-15 and ~7-13, respectively, times higher as compared to those of the pure Au electrode.

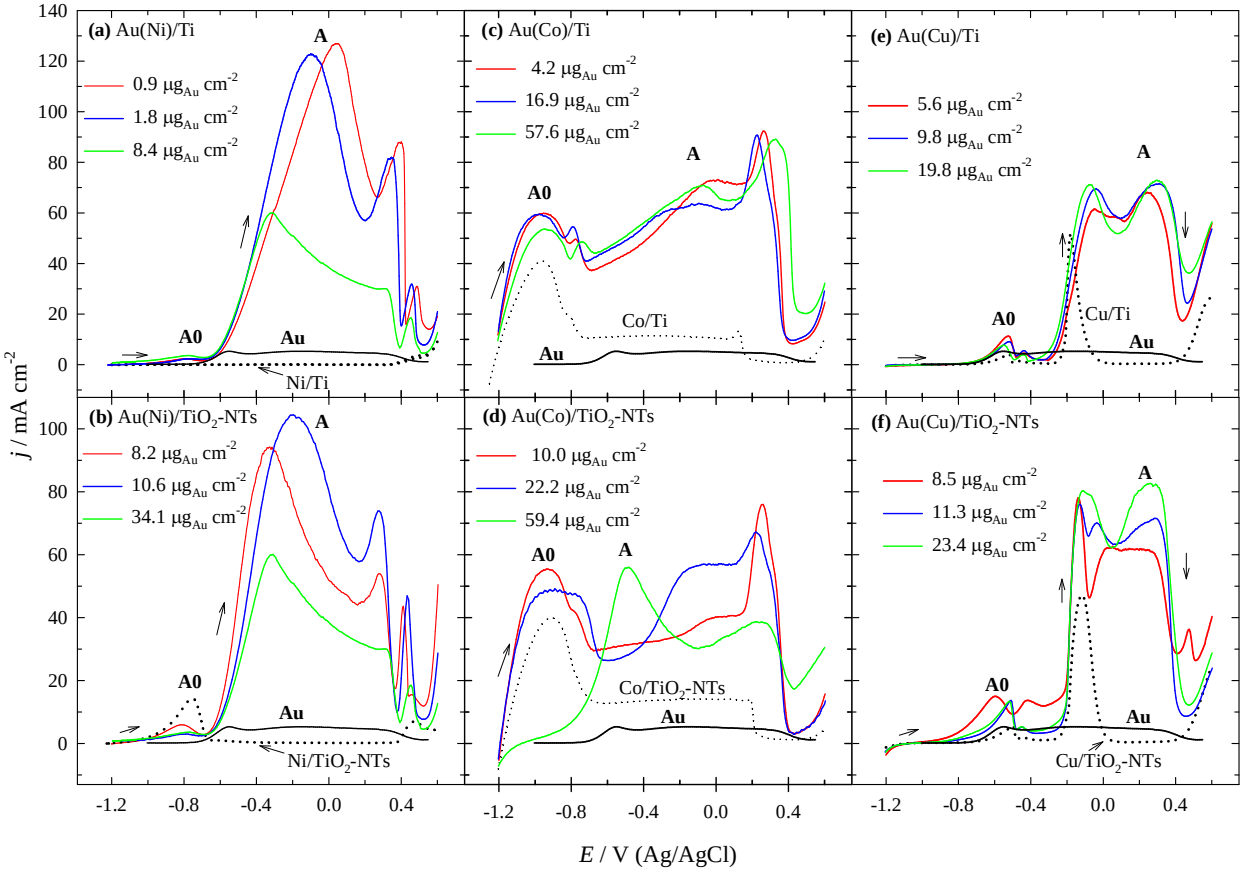

Fig. 9. Positive going scans of BH_4^- oxidation recorded on the Au (a,b), M/Ti, M/TiO_2-NTs, Au(M)/Ti and Au(M)/TiO_2-NTs catalysts with different Au loadings in 0.05 M $NaBH_4$ + 1 M NaOH at 10 mV s^{-1}; 25 ºC.

Once the oxidation of BH_4^- ions on the latter catalysts is compared, it is seen that the highest current densities are observed on the Au(Ni)/Ti catalyst with a lower Au loading of 0.9 $\mu g_{Au}\,cm^{-2}$ (Fig. 9 a). With increase in Au loading up to 8.4 $\mu g_{Au}\,cm^{-2}$ on the Ni/Ti electrode the potential values of peak **A** are shifted to negative potential values. To compare the electrocatalytic activity of these catalysts, the current density was normalized in reference to the Au loadings for each catalyst to represent the mass activity of catalysts towards the oxidation of sodium borohydride.

The Au mass peak current (peak **A**) of the Au(Ni)/Ti catalyst with the Au loading of 0.9 $\mu g_{Au} cm^{-2}$ is 2.1-14.3 times higher than those on the Au(Ni)/Ti catalysts with the Au loadings of 1.8 and 8.4 $\mu g_{Au} cm^{-2}$, respectively. The Au mass peak current (peak **A**) of the Au(Ni)/TiO_2-NTs catalyst with the Au loading of 8.2 $\mu g_{Au} cm^{-2}$ is 1.2-6.5 times higher than those on the Au(Ni)/TiO_2-NTs catalysts with the Au loadings of 10.6 and 34.1 $\mu g_{Au} cm^{-2}$, respectively. The higher mass specific current density have been obtained on the Ti surface. The Au mass peak current (peak **A**) of the Au(Ni)/Ti catalyst with the Au loading of 0.9 $\mu g_{Au} cm^{-2}$ is 12.2 times higher than those on the Au(Ni)/TiO_2-NTs catalyst with the Au loading of 8.2 $\mu g_{Au} cm^{-2}$.

The electrochemical behavior of the Co/Ti, Co/TiO_2-NTs, Au(Co)/Ti and Au(Co)/TiO_2-NTs catalysts towards the oxidation of BH_4^- ions was also evaluated in an alkaline medium using the cyclic voltammetry method (Fig. 9 c,d). During the anodic scan in contrast to the oxidation of BH_4^- on the bare Au electrode (Fig. 7), two well-expressed anodic peaks: peak **A0** at lower potential values and peak **A** at more positive potential values are seen in the anodic scans for the as-prepared Co/Ti, Co/TiO_2-NTs, Au(Co)/Ti and Au(Co)/TiO_2-NTs catalysts (Fig. 9 c,d). Oxidation peak **A** that is related to the direct oxidation of BH_4^- ions recorded on the Au(Co)/Ti and Au(Co)/TiO_2-NTs catalysts appears in the same potential region as on the pure Au electrode indicating a high activity of the latter catalysts. It should be noted that the both oxidation peaks recorded on the Au(Co)/Ti and Au(Co)/TiO_2-NTs catalysts are higher than those recorded on Co/Ti or Co/TiO_2-NTs. An enhanced electrocatalytic activity of the as-prepared Au(Co)/Ti and Au(Co)/TiO_2-NTs catalysts can be ascribed to the intrinsic electrocatalytic activity of the Au nanoparticles deposited on the Co/Ti surface and formation of AuCo alloy as was confirmed by XRD analysis (Fig. 6 c). Wide oxidation waves recorded both on bare Au and the Au(Co)/Ti catalysts, which extend up to 0.4 V, correspond to the oxidation of the reaction intermediates on the partially oxidized Au surface. It can be noted that the Au(Co)/TiO_2-NTs electrode with the Au loading of 59 $\mu g_{Au} cm^{-2}$ and the bare Au electrode has the same potential value of oxidation peak **A** (ca. -0.5 V, Fig. 9 d), the peak current

density being ca. 7 times higher than that of pure Au. Additionally, the Au(Co)/TiO_2-NTs electrode with the highest Au loading of 59 $\mu g_{Au} cm^{-2}$ shows an almost negligible anodic peak **A0**, probably as a result of the lower Co content on the surface of this electrode (Table IV). Furthermore, the CV profile of Au(Co)/TiO_2-NTs (59 $\mu g_{Au} cm^{-2}$) in the potential region from ca. -0.7 V to 0.4 V (Fig. 9 d) showed characteristics similar to that of pure Au in the alkaline borohydride solution (Fig. 7). It is worth noting that this potential region is in the vicinity of that of Au monolayer formation on the Co/TiO_2-NTs surface. It is clear that the Au mass specific peak current density of the Au(Co)/TiO_2-NTs catalyst with the Au loading of 10 $\mu g_{Au} cm^{-2}$ is higher than that of the Au(Co)/TiO_2-NTs catalysts with the Au loadings of 22 and 59 $\mu g_{Au} cm^{-2}$, respectively. The Au mass peak current (peak **A**) of the Au(Co)/Ti catalyst with the Au loading of 4.2 $\mu g_{Au} cm^{-2}$ is 4-14 times higher than those on the Au(Co)/Ti catalysts with the Au loadings of 16.9 and 57.6 $\mu g_{Au} cm^{-2}$, respectively. This phenomenon could be explained by the size of Au nanoparticles, i.e. when the Au loading on the Co/Ti or Co/TiO_2-NTs is the lowest, the size of Au nanoparticles is also the smallest one compared with higher Au loadings deposited on the Co/Ti or Co/TiO_2-NTs surfaces (Fig. 4). Mass specific peak current density is ca. 3.2 times higher using Au(Co)/Ti catalyst with the Au loading of 4.2 $\mu g_{Au} cm^{-2}$ than that of the Au(Co)/TiO_2-NTs catalyst with the Au loading of 10 $\mu g_{Au} cm^{-2}$.

Figure 9 (e and f) shows stabilized anodic scans (5^{th} cycles) of the oxidation of BH_4^- ions recorded on Cu/Ti, Cu/TiO_2-NTs and different Au(Cu)/Ti and Au(Cu)/TiO_2-NTs catalysts. Since the Cu/Ti or Cu/TiO_2-NTs electrodes do not show electroactivity towards the direct electrooxidation of BH_4^- ions (Fig. 9 e,f), the observed prominent anodic currents under the potential region of -0.4 and 0.5 V can be ascribed to the electrocatalytic activity of Au nanoparticles deposited on the Cu/Ti or Cu/TiO_2-NTs electrodes. Noteworthy, the current densities of peak **A** on the Au(Cu)/Ti and Au(Cu)/TiO_2-NTs catalysts are ca. 7.7-8.9 and 10-fold, respectively, higher compared to those on pure Au.

The Au mass peak current (peak **A**) of the Au(Cu)/Ti catalyst with the Au loading of 5.6 $\mu g_{Au} cm^{-2}$ is ca. 1.5-3 times higher than those on the Au(Cu)/Ti catalysts with the Au loadings of 9.8 and 19.8 $\mu g_{Au} cm^{-2}$, respectively. The Au mass peak current (peak **A**) of the

Au(Cu)/TiO_2-NTs catalyst with the Au loading of 8.5 $\mu g_{Au} cm^{-2}$ is ca. 1.4-2.7 times higher than those on the Au(Cu)/TiO_2-NTs catalysts with the Au loadings of 11.3 and 23.4 $\mu g_{Au} cm^{-2}$, respectively. A higher mass specific current density was obtained on the Ti surface. The Au mass peak current (peak **A**) of the Au(Cu)/Ti catalyst with the Au loading of 5.6 $\mu g_{Au} cm^{-2}$ is ca. 1.2 times higher than that on the Au(Cu)/TiO_2-NTs catalyst with the Au loading of 8.5 $\mu g_{Au} cm^{-2}$.

The current density of the Au(Ni)/Ti catalyst with the Au loading of 0.9 $\mu g_{Au} cm^{-2}$ is 1.3 and 2.0 times higher than those on the Au(Co)/Ti and Au(Cu)/Ti catalysts with the Au loadings of 4.2 and 5.6 $\mu g_{Au} cm^{-2}$, respectively. The current density of the Au(Ni)/TiO_2-NTs catalyst with the Au loading of 8.2 $\mu g_{Au} cm^{-2}$ is 1.2 and 1.5 times higher than those on the Au(Co)/TiO_2-NTs and Au(Cu)/TiO_2-NTs catalysts with the Au loadings of 10.0 and 8.5 $\mu g_{Au} cm^{-2}$, respectively.

Au(M)/Ti and Au(Cu)/TiO_2-NTs (M = Ni, Co, Cu) catalysts have an enhanced electrocatalytic activity towards the oxidation of sodium borohydride as compared with that of pure Au, M/Ti and M/TiO_2-NTs. The highest catalytic activity was obtained using the catalysts with a Ni sublayer deposited on the Ti or TiO_2-NTs surfaces. The fabricated Au(M)/Ti and Au(M)/TiO_2-NTs catalysts seem to be a promising anodic material for direct borohydride fuel cells.

3.3. $NaBH_4$-H_2O_2 fuel cell test experiments

Direct alkaline $NaBH_4$-H_2O_2 single fuel cell tests were carried out by employing the prepared M/Ti, M/TiO_2-NTs, Au(M)/Ti and Au(M)/TiO_2-NTs catalysts (with a geometric area of 2 cm^2) as the anode and a Pt sheet as the cathode. The anolyte was composed of an alkaline mixture of 1 M $NaBH_4$ + 4 M NaOH and the catholyte contained 5 M H_2O_2 + 1.5 M HCl at temperatures of 25-55 ºC. The performance of the fuel cell was evaluated by recording the cell polarization and obtaining the corresponding power density curves. Figure 10 presents the fuel cell polarization curves and the corresponding power densities against the current density by employing the M/Ti, M/TiO_2-NTs, Au(M)/Ti and Au(M)/TiO_2-NTs catalysts at a temperature of 25 ºC. Notably, peak power density values increase with the

increase in DBHPFC temperature and are greater when using Au(M)/Ti or Au(M)/TiO_2-NTs catalysts as anode material as compared with those of M/Ti or M/TiO_2-NTs. During the cell discharge process, small bubbles of hydrogen and oxygen were observed at the electrodes surface due to the chemical decomposition of BH_4^- and H_2O_2 at the anode and at the cathode, respectively. The fuel cell displayed an open circuit voltage of ca. 1.9 V using catalysts with a Ni or Co sublayer on the Ti and TiO_2-NTs surfaces and ca. 1.6 V using catalysts with a Cu sublayer on the Ti and TiO_2-NTs surfaces.

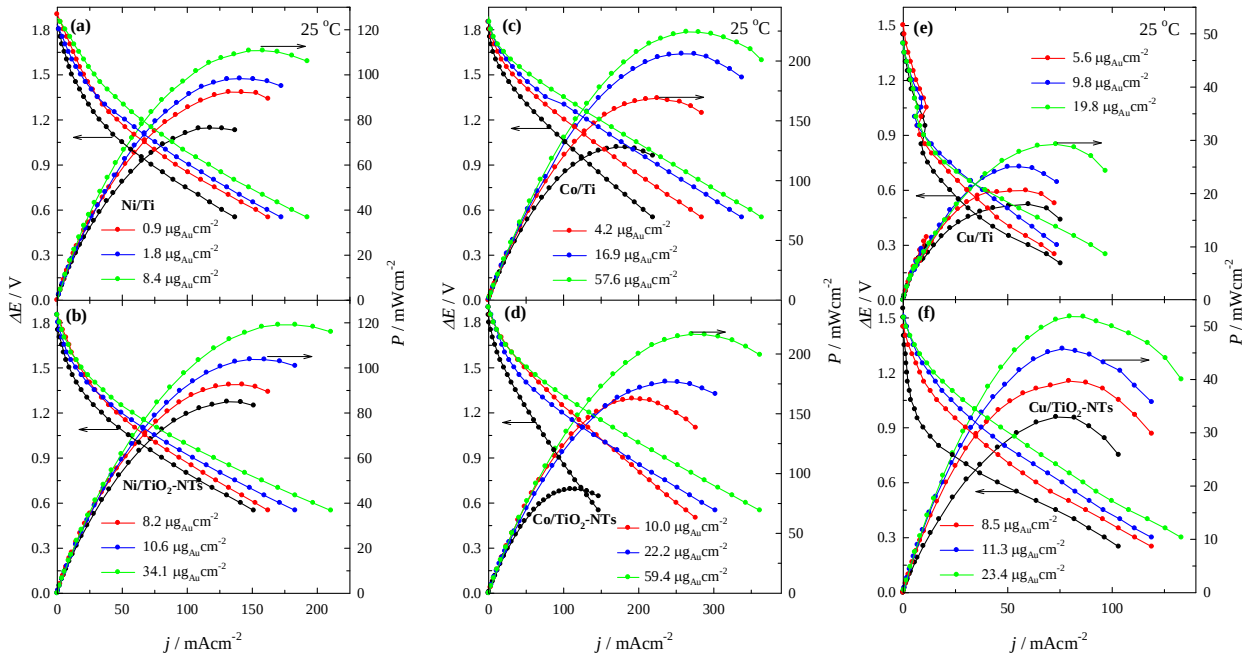

Fig. 10. Cell polarization and power density curves for the DBHPFC using M/Ti, M/TiO_2-NTs, Au(M)/Ti and Au(M)/TiO_2-NTs anode catalysts with anolyte consisted of 1 M $NaBH_4$ + 4 M NaOH and 5 M H_2O_2 + 1.5 M HCl catholyte at 25 ºC.

As seen, the M/Ti and M/TiO_2-NTs electrodes generate the maximum power density of ca. 18-128 and 33-87 mW cm^{-2}, respectively, at 25 ºC. Peak power densities up to 128 mW cm^{-2} were attained at 25 ºC at a current density of 171 mA cm^{-2} and a cell voltage of 0.75 V using the Co/Ti electrode (Table V) and it is ~1.7 and 7.1 times higher than the power densities obtained using Ni/Ti and Cu/Ti electrodes under the same conditions (Table V). Peak power densities up to 87 mW cm^{-2} were attained at 25 ºC at a current density of 109 mA cm^{-2} and a cell voltage of 0.8 V using the Co/TiO_2-NTs electrode and it

is ~1 and 2.6 times higher than the power densities obtained using Ni/TiO_2-NTs and Cu/TiO_2-NTs electrodes under the same conditions (Table V). The peak power densities are 1.5-1.7 times higher with a Co sublayer on the Ti surface than those on the TiO_2-NTs surface at temperatures of 25-55 ºC.

The electrochemical parameters of DBHPFCs using different Au(M)/Ti and Au(M)/TiO_2-NTs anode catalysts are shown in Tables VI-VIII. The Au(Ni)/Ti and Au(Ni)/TiO_2-NTs generate the maximum power density of ca. 92-162 and 93-167 mW cm^{-2}, respectively, at temperatures of 25-55 ºC. Peak power densities up to 93 mW cm^{-2} were attained at 25 ºC at a current density of 142 mA cm^{-2} and a cell voltage of 0.65 V using the Au(Ni)/TiO_2-NTs catalyst with the Au loading of 8.2 $\mu g_{Au} cm^{-2}$ (Table VI). The Au(Co)/Ti and Au(Co)/TiO_2-NTs generate the maximum power density of ca. 169-288 and 163-283 mW cm^{-2}, respectively, at temperatures of 25-55 ºC. Peak power densities up to 169 mW cm^{-2} were attained at 25 ºC at a current density of 225 mA cm^{-2} and a cell voltage of 0.75 V using the Au(Co)/Ti catalyst with the Au loading of 4.2 $\mu g_{Au} cm^{-2}$ (Table VII). The Au(Cu)/Ti and Au(Cu)/TiO_2-NTs generate a peak power density of ca. 21-38 and 40-92 mW cm^{-2}, respectively, at temperatures of 25-55 ºC.

TABLE V. Electrochemical parameters of DBHPFCs using the M/Ti, M/TiO_2-NTs (M=Ni, Co, Cu) anode catalysts.

Catalyst	**T (ºC)**	**Peak power density (mW cm^{-2})**	***j* at peak power density (mA cm^{-2})**	***E* at peak power density (V)**
Ni/Ti	25	76.4	117.5	0.65
	35	92.4	131.9	0.70
	45	103.3	147.5	0.70
	55	109.3	128.4	0.85
Ni/TiO_2-NTs	25	85.0	130.6	0.65
	35	92.7	142.5	0.65
	45	106.5	163.7	0.65
	55	120.8	172.5	0.70
Co/Ti	25	128.0	170.6	0.75
	35	141.6	188.7	0.75
	45	157.1	209.3	0.75
	55	177.1	221.2	0.80
Co/TiO_2-NTs	25	87.0	108.7	0.80
	35	89.1	118.7	0.75
	45	94.2	125.6	0.75
	55	101.7	135.6	0.75
Cu/Ti	25	18.0	60.0	0.30
	35	22.7	64.7	0.35
	45	24.6	61.4	0.40
	55	27.0	67.5	0.40
Cu/TiO_2-NTs	25	33.0	73.2	0.45
	35	41.2	82.3	0.50
	45	44.4	80.6	0.55
	55	54.9	84.4	0.65

TABLE VI. Electrochemical parameters of DBHPFCs using different Au(Ni)/Ti, Au(Ni)/TiO_2-NTs anode catalysts.

Catalyst	Au loading ($\mu g_{Au} cm^{-2}$)	T (ºC)	Peak power density (mW cm^{-2})	*j* at peak power density (mA cm^{-2})	*E* at peak power density (V)	Specific peak power density (mW μg_{Au}^{-1})
Au(Ni)/Ti	0.9	25	92.3	131.8	0.70	102.6
		35	104.2	148.7	0.70	115.8
		45	114.3	163.1	0.70	127.0
		55	123.5	176.2	0.70	137.2
	1.8	25	98.3	140.4	0.70	54.6
		35	113.4	174.3	0.65	63.0
		45	128.2	197.2	0.65	71.2
		55	134.9	192.5	0.70	74.9
	8.4	25	110.7	158.1	0.70	13.2
		35	128.2	197.2	0.65	15.3
		45	143.1	220.0	0.65	17.0
		55	161.8	215.6	0.75	19.3
Au(Ni)/TiO_2-NTs	8.2	25	92.6	142.3	0.65	11.3
		35	108.1	166.2	0.65	13.2
		45	122.8	175.3	0.70	15.0
		55	131.1	187.2	0.70	16.0
	10.6	25	103.8	148.1	0.70	9.8
		35	119.5	170.6	0.70	11.3
		45	130.2	185.9	0.70	12.3
		55	147.0	195.9	0.75	13.9
	34.1	25	119.1	183.1	0.65	3.5
		35	135.1	180.0	0.75	4.0
		45	149.3	186.5	0.80	4.4
		55	166.9	196.2	0.85	4.9

TABLE VII. Electrochemical parameters of DBHPFCs using different Au(Co)/Ti, Au(Co)/TiO_2-NTs anode catalysts.

Catalyst	**Au loading ($\mu g_{Au} cm^{-2}$)**	T (^oC)	**Peak power density ($mW\ cm^{-2}$)**	***j* at peak power density ($mA\ cm^{-2}$)**	***E* at peak power density (V)**	**Specific peak power density** ($mW\ \mu g_{Au}^{-1}$)
Au(Co)/Ti	4.2	25	168.8	225.0	0.75	40.2
		35	182.3	214.3	0.85	43.4
		45	195.1	229.3	0.85	46.5
		55	200.6	250.6	0.80	47.8
	16.9	25	206.1	257.5	0.80	12.2
		35	228.6	285.6	0.80	13.5
		45	244.6	305.6	0.80	14.5
		55	259.9	305.6	0.85	15.4
	57.6	25	224.3	263.7	0.85	3.9
		35	256.2	301.2	0.85	4.5
		45	277.5	326.2	0.85	4.8
		55	288.1	338.7	0.85	5.0
Au(Co)/TiO_2-NTs	10.0	25	162.6	191.2	0.85	16.3
		35	178.0	209.3	0.85	17.8
		45	191.5	239.3	0.8	19.2
		55	204.0	254.9	0.8	20.4
	22.2	25	176.8	235.6	0.75	8.0
		35	189.5	252.4	0.75	8.5
		45	218.1	272.4	0.8	9.8
		55	258.1	322.4	0.8	11.6
	59.4	25	216.6	270.6	0.8	3.7
		35	239.1	298.7	0.8	4.0
		45	262.0	308.0	0.85	4.4
		55	283.3	333.0	0.85	4.8

TABLE VIII. Electrochemical parameters of DBHPFCs using different Au(Cu)/Ti, Au(Cu)/TiO_2-NTs anode catalysts.

Catalyst	**Au loading ($\mu g_{Au} cm^{-2}$)**	T (^oC)	**Peak power density ($mW\ cm^{-2}$)**	***j* at peak power density ($mA\ cm^{-2}$)**	***E* at peak power density (V)**	**Specific peak power density** ($mW\ \mu g_{Au}^{-1}$)
Au(Cu)/Ti	5.6	25	20.6	58.7	0.35	3.7
		35	23.8	59.4	0.40	4.3
		45	26.6	66.4	0.40	4.8
		55	29.4	73.5	0.40	5.3
	9.8	25	25.1	55.6	0.45	2.6
		35	27.2	60.4	0.45	2.8
		45	29.4	73.4	0.40	3.0
		55	33.7	84.1	0.40	3.4
	19.8	25	29.3	73.1	0.40	1.5
		35	31.7	79.1	0.40	1.6
		45	34.1	85.1	0.40	1.7
		55	38.0	94.8	0.40	1.9
Au(Cu)/TiO_2-NTs	8.5	25	39.7	79.3	0.50	4.7
		35	45.3	90.5	0.50	5.3
		45	51.3	93.1	0.55	6.0
		55	62.6	89.4	0.70	7.4
	11.3	25	45.8	76.2	0.60	4.1
		35	54.7	99.4	0.55	4.8
		45	62.6	104.3	0.60	5.5
		55	71.7	119.5	0.60	6.3
	23.4	25	51.8	79.7	0.65	2.2
		35	63.8	98.1	0.65	2.7
		45	80.8	134.7	0.60	3.5
		55	91.9	153.1	0.60	3.9

Peak power densities up to 40 $mW\ cm^{-2}$ were attained at 25 ºC at a current density of 79 $mA\ cm^{-2}$ and a cell voltage of 0.5 V using the Au(Cu)/TiO_2-NTs catalyst with the Au loading of 8.5 $\mu g_{Au} cm^{-2}$ (Table VIII). Peak power density is 1.8 and 8.2 times higher at 25 ºC using the Au(Co)/Ti catalyst after immersion into the gold-containing solution for

0.5 min than using the Au(Ni)/Ti and Au(Cu)/Ti catalysts, respectively, under the same conditions. Peak power density is 1.8 and 4.1 times higher at 25 ºC using the Au(Co)/TiO_2-NTs catalyst after immersion into the gold-containing solution for 0.5 min than Au(Ni)/TiO_2-NTs and Au(Cu)/TiO_2-NTs catalysts, respectively, under the same conditions.

To compare the catalytic activity of the Au(M)/Ti and Au(M)/TiO_2-NTs catalysts, the peak power density values were normalized in reference to the Au loadings for each catalyst, i.e. the power density per microgram of Au and are given in Tables VI-VIII. It is clear that the Au specific peak power density of the Au(M)/Ti and Au(M)/TiO_2-NTs catalysts with the lowest Au loadings is higher than that of the catalysts with higher Au loadings. The highest specific peak power densities of 102.6 mW μg_{Au}^{-1} at 25 °C were attained using the Au(Ni)/Ti anode with the Au loading of 0.9 μg cm^{-2} and of 16.3 mW μg_{Au}^{-1} at 25 °C were attained using the Au(Ni)/TiO_2-NTs anode with the Au loading of 10.0 μg cm^{-2}.

Direct alkaline $NaBH_4$-H_2O_2 single fuel cell tests were carried out by employing the prepared M/Ti, M/TiO_2-NTs, Au(M)/Ti and Au(M)/TiO_2-NTs catalysts at temperatures of 25-55 ºC. It was found that the highest peak power densities up to 224 mW cm^{-2} were attained at 25 ºC using the Au(Co)/Ti catalyst, with the Au loading of 57.6 μg cm^{-2}. The highest specific peak power densities of 102.6 mW μg_{Au}^{-1} at 25 °C were attained using the Au(Ni)/Ti anode with the Au loading of 0.9 μg cm^{-2}.

CONCLUSIONS

1. The Au(M)/Ti and Au(M)/TiO_2-NTs (M = Ni, Cu, Co) catalysts were prepared by means of the electroless metal deposition and galvanic displacement techniques. It has been found that:

a) with the aim of formation of effective catalysts, the immobilization of Au nanoparticles should be made on the underlayers deposited on the Ti and TiO_2-NTs surfaces with the thickness of ca. 0.2-0.4 μm for Ni, ca. 0.5-1.1 μm for Co and ca. 1.5 μm for Cu;

b) the optimal time period of immersion for Au deposition varies from 0.5 to 5 minutes. Due to spontaneous displacement of metal by gold, the Au(M)/Ti Au(M)/TiO_2-NTs catalysts were fabricated with the Au nanoparticles sized ca. 10-100 nm and having the Au loadings from ca. 0.9 to 59.4 $\mu g_{Au}\,cm^{-2}$.

2. The prepared Au(M)/Ti and Au(M)/TiO_2-NTs catalysts have a significantly higher electrocatalytic activity towards the oxidation of sodium borohydride as compared to that of the bare Au, M/Ti and M/TiO_2-NTs electrodes. The Au(M)/Ti catalysts with the Au loading from 0.9 to 57.6 $\mu g_{Au}\,cm^{-2}$, and the Au(M)/TiO_2-NTs catalysts with the Au loading from 8.2 to 59.4 $\mu g_{Au}\,cm^{-2}$ exhibit ca. 7-16 times higher electrocatalytic activity towards the electrooxidation reaction of sodium borohydride in an alkaline medium as compared with that of bare Au electrode. The highest mass activity (140 mA μg_{Au}^{-1}) towards the oxidation reaction of sodium borohydride was obtained on the Au(Ni)/Ti catalyst with the Au loading of 0.9 $\mu g_{Au}\,cm^{-2}$.

3. Direct alkaline $NaBH_4$-H_2O_2 single fuel cell tests were carried out by employing the prepared M/Ti, M/TiO_2-NTs, Au(M)/Ti and Au(M)/TiO_2-NTs catalysts as the anodes. It has been found that the highest peak power density up to 224 $mW\,cm^{-2}$ was attained at a temperature of 25 ºC using the Au(Co)/Ti catalyst with the Au loading of 57.6 $\mu g\,cm^{-2}$ as the anode. The highest specific peak power density of 102.6 $mW\,\mu g_{Au}^{-1}$ at a temperature of 25 °C was attained using Au(Ni)/Ti with the Au loading of 0.9 $\mu g\,cm^{-2}$ as an anode.

4. The Au(M)/Ti and Au(M)/TiO_2-NTs catalysts are promising materials and can be used as anodes in direct sodium borohydride fuel cells.

List of Publications

ISI Referred Journals

1. **A. Balčiūnaitė**, L. Tamašauskaitė-Tamašiūnaitė, D.M.F. Santos, A. Zabielaitė, A. Jagminienė, I. Stankevičienė, E. Norkus. "*Gold-cobalt deposited on titania nanotubes as anode catalyst for direct borohydride fuel cells*". Fuel Cells (*awaiting decision*).

2. D. M. F. Santos, **A. Balčiūnaitė**, L. Tamašauskaitė-Tamašiūnaitė, A. Zabielaitė, A. Jagminienė, I. Stankeviciene, A. Naujokaitis, E. Norkus. "*AuCo/TiO_2-NTs anode catalysts for direct borohydride fuel cells*". J. Electrochem. Soc. 163(14) (2016) F1553-F1557.

3. L. Tamašauskaitė-Tamašiūnaitė, J. Rakauskas, **A. Balčiūnaitė**, A. Zabielaitė, J. Vaičiūnienė, A. Selskis, E. Norkus. "*Nanostructured gold-nickel/titania nanotubes electrocatalysts for hydrazine oxidation*". J. Power Sources 272 (2014) 362-370.

4. L. Tamašauskaitė-Tamašiūnaitė, **A. Balčiūnaitė**, A. Zabielaitė, I. Stankevičienė, V. Kepenienė, A. Selskis, R. Juškėnas, E. Norkus. "*Investigation of electrocatalytic activity of the nanostructured Au-Cu catalyst deposited on the titanium surface towards borohydride oxidation*". J. Electroanal. Chem. 700 (2013) 1-7.

5. L. Tamašauskaitė-Tamašiūnaitė, A. Jagminienė, **A. Balčiūnaitė**, A. Zabielaitė, A. Žielienė, L. Naruškevičius, J. Vaičiūnienė, A. Selskis, R. Juškėnas, E. Norkus. "*Electrocatalytic activity of the nanostructured Au-Co catalyst deposited onto titanium towards borohydride oxidation*". Int. J. Hydrogen Energy 38 (2013) 14232-14241.

6. L. Tamašauskaitė-Tamašiūnaitė, **A. Balčiūnaitė**, D. Šimkūnaitė, A. Selskis. "*Self-ordered titania nanotubes and flat surfaces as a support for deposition of Au-Ni catalyst: Enhanced electrocatalytic oxidation of borohydride*". J. Power Sources 202 (2012) 85-91.

7. L. Tamašauskaitė-Tamašiūnaitė, **A. Balčiūnaitė**, R. Čekavičiūtė, A. Selskis. "*Investigation of titanium supported nanostructured Au-Ni and Pt-Ni thin layers as electrocatalysts for DBFC*". J. Electrochem. Soc. 159 (2012) B611-B618.

Other Referred International Journals

8. D. M. F. Santos, **A. Balčiūnaitė**, L. Tamašauskaitė-Tamašiūnaitė, A. Zabielaitė, A. Jagminienė, I. Stankevičienė, E. Norkus. "*Gold-cobalt deposited on titania nanotubes as anode catalyst for direct borohydride fuel cells*". ECS Transactions 72 (25) (2016) 65-71.

9. L. Tamašauskaitė-Tamašiūnaitė, A. Jagminienė, **A. Balčiūnaitė**, A. Zabielaitė, A. Selskis, E. Norkus. "*Electrocatalytic activity of the nanostructured Au-Co catalysts deposited on the titanium towards borohydride oxidation*". ECS Transactions 53(23) (2013) 43-54.

10. L. Tamašauskaitė-Tamašiūnaitė, **A. Balčiūnaitė**, A. Vaiciukevičienė, I. Stankevičienė, A. Selskis, E. Norkus. "*Investigation of electrocatalytic activity of the nanostructured Au-Cu catalyst deposited on the titanium surface towards borohydride oxidation*". ECS Transactions 50(2) (2012) 1987-1995.

Conference Materials

Thesis of International Conferences

1. **A. Balčiūnaitė**, L. Tamašauskaitė-Tamašiūnaitė, D. M. F. Santos, A. Zabielaitė, I. Stankevičienė, A. Jagminienė, E. Norkus. "*Gold-metal (Ni, Cu, Co) deposited on titania nanotubes as electrocatalysts for direct borohydride fuel cell*". 4th International Symposium on Energy Efficiency and Energy Related Materials, ENEFM2017: Oludeniz, Turkey (2017) ID-46.

2. D. M. F. Santos, **A. Balčiūnaitė**, L. Tamašauskaitė-Tamašiūnaitė, A. Zabielaitė, A. Jagminienė, I. Stankeviciene, E. Norkus. "*Gold-cobalt deposited on titania nanotubes as anode catalyst for direct borohydride fuel cells*". 229th ECS Meeting: San Diego, USA (2016) I05-1572.

3. **A. Balčiūnaitė**, L. Tamašauskaitė-Tamašiūnaitė, A. Jagminienė, A. Matusevičiūtė, A. Selskis, E. Norkus. "*Gold-cobalt/titania nanotubes electrocatalysts for borohydride oxidation*". 3rd ENEFM2015, International Congress on Energy Efficiency and Energy Related Materials: Oludeniz, Turkey (2015) ID 19.

4. L. Tamašauskaitė-Tamašiūnaitė, **A. Balčiūnaitė**, A. Zabielaitė, I. Stankevičienė, A. Jagminienė, E. Norkus. "*Direct borohydride fuel cells employing gold or platinum-metal (Ni, Cu) deposited on titanium catalysts*". 3rd ENEFM2015, International Congress on Energy Efficiency and Energy Related Materials: Oludeniz, Turkey (2015) ID 4.

5. **A. Balčiūnaitė**, I. Stankevičienė, A. Zabielaitė, J. Vaičiūnienė, A. Selskis, R. Juškėnas, L. Tamašauskaitė-Tamašiūnaitė, E. Norkus. "*Gold-metal (Ni, Cu) deposited on the titania as electrocatalysts for borohydride oxidation*". 226th ECS and SMEQ Joint International Meeting: Cancun, Mexico (2014) F3-1127 (**oral**).

6. L. Tamašauskaitė-Tamašiūnaitė, J. Rakauskas, **A. Balčiūnaitė**, A. Zabielaitė, J. Vaičiūnienė, A. Selskis, E. Norkus. "*Nanostructured gold-nickel/titania nanotubes electrocatalysts for hydrazine oxidation*". 225th ECS Meeting: Orlando, USA (2014) E5-597.

7. L. Tamašauskaitė-Tamašiūnaitė, **A. Balčiūnaitė**, A. Zabielaitė, I. Stankevičienė, A. Jagminienė, V. Kepenienė, A. Selskis, R. Juškėnas, E. Norkus. "*Comparative study of electrocatalytic activity towards borohydride oxidation on gold- or platinum-metal (Cu, Co, Ni) deposited on the titanium surface via galvanic displacement*". 225th ECS Meeting: Orlando, USA (2014) E5-607 (**oral**).

8. L. Tamašauskaitė-Tamašiūnaitė, I. Balčiūnaitė, **A. Balčiūnaitė**, A. Zabielaitė, I. Stankevičienė, A. Jagminienė, V. Kepenienė, J. Vaičiūnienė, A. Selskis, R. Juškėnas, E. Norkus. "*Investigation of borohydride oxidation on gold-metal (Cu, Co, Ni) deposited on the titanium surface via galvanic displacement*". 15-th International Conference-School Advanced Materials and technologies: Palanga, Lithuania (2013) P118, p. 165.

9. **A. Balčiūnaitė**, L. Tamašauskaitė-Tamašiūnaitė. "*Investigation of kinetics of sodium borohydride oxidation on nanostructured gold-nickel catalyst deposited on the titania nanotubes*". Chemistry and chemical technology of inorganic materials: proceedings of scientific conference "Chemistry and chemical technology" (2013), Kaunas, Lithuania, p. 32-37.

10. L. Tamašauskaitė-Tamašiūnaitė, A. Jagminienė, **A. Balčiūnaitė**, A. Zabielaitė, A. Selskis, E. Norkus. "*Electrocatalytic activity of the nanostructured Au(Co)/Ti catalysts towards borohydride oxidation*". 223rd ECS Meeting: Toronto, Canada (2013) 382.

11. L. Tamašauskaitė-Tamašiūnaitė, **A. Balčiūnaitė**, A. Vaiciukevičienė, I. Stankevičienė, A. Selskis, E. Norkus. "*Investigation of electrocatalytic activity of the nanostructured Au-Cu catalyst deposited on the titanium surface towards borohydride oxidation*". 222nd ECS Meeting: Honolulu, Hawaii (USA) (2012) B9-1455.

Thesis of National Conferences

12. **A. Balčiūnaitė**, L. Tamašauskaitė-Tamašiūnaitė. "*Borhidrido oksidacijos ant Au(Ni)/TiO$_2$nv ir Au(Cu)/TiO$_2$nv katalizatorių tyrimas*". 4 Fizinių ir technologijos mokslų centro doktorantų ir jaunųjų mokslininkų konferencija (FizTech): Vilnius, (2014) P. 1 (**oral**).

13. **A. Balčiūnaitė**, L. Tamašauskaitė-Tamašiūnaitė. "*Borhidrido oksidacijos tyrimas ant nanostruktūrizuoto Au-Cu katalizatoriaus, nusodinto ant titano oksido nanovamzdelių paviršiaus*". Trečioji jaunųjų mokslininkų konferencija, Fizinių ir technologijos mokslų tarpdalykiniai tyrimai: Vilnius (Lietuva) (2013) (**oral**).

Awards

2013 - Laureate of the Conference of Young Researchers, organized by Lithuanian Academy of Sciences.

2013 - INFOBALT award for the study "*Investigation of borohydride oxidation at the nanostructured Au-Cu deposited on the titania nanotube arrayed surface*".

2013 - Lithuanian Academy of Sciences award for the best student study "*Investigation of borohydride oxidation at the nanostructured Au(Ni)/TiO$_2$-NTs electrode*".

NAUJOS MEDŽIAGOS ŠARMINIAMS KURO ELEMENTAMS: SINTEZĖ, CHARAKTERIZAVIMAS IR SAVYBĖS

Santrauka

Alternatyvių energijos šaltinių paiešką lemia didėjantis energijos poreikis bei senkantys tradiciniai energijos šaltiniai bei resursai. Kuro elementas cheminės reakcijos energiją tiesiogiai verčia elektros energija. Kuro elementai kol kas yra švariausias žinomas elektros energijos gavimo būdas. Disertacinis darbas susietas su perspektyviais, visame pasaulyje intensyviai vykdomais kuro elementuose naudojamų medžiagų savybių tyrimais ir yra skirtas naujų efektyvių medžiagų paieškai, kurias galima pritaikyti tiesioginių natrio borohidrido kuro elementų sukūrimui, siekiant padidinti esamų ar naujų kuro elementų našumą. Taigi šio darbo tikslas buvo efektyvių katalizatorių formavimas, apibūdinimas bei taikymas tiesioginiuose natrio borohidrido kuro elementuose.

Šio darbo metu buvo formuojami daugiafunkciniai M/Ti, M/TiO_2nv, Au(M)/Ti ir Au(M)/TiO_2nv (M = Ni, Co, Cu) katalizatoriai, taikant paprastus bei santykinai nebrangius cheminio metalų nusodinimo ir galvaninio pakeitimo metodus. Nustatyta, kad efektyvių katalizatorių formavimui, Au nanodalelių imobilizavimui ant Ti ir TiO_2nv paviršiaus, turi būti nusodinamas apie 0,2-0,4 µm storio Ni pasluoksnis, ~0,5-1,1 µm storio Co pasluoksnis ir apie 1,5 µm storio Cu pasluoksnis, o optimalus imersinio Au nusodinimo laikas – 0,5-5 min. Nusodinto Au nanodalelių dydis yra nuo 10-100 nm, o nusodinto Au įkrova yra 0,9-59,4 $\mu g_{Au}\,cm^{-2}$ suformuotuose Au(M)/Ti bei Au(M)/TiO_2nv katalizatoriuose. Sukurti Au(M)/Ti ir Au(M)/TiO_2nv katalizatoriai pasižymi itin dideliu elektrokataliziniu aktyvumu natrio borohidrido oksidacijos reakcijai, palyginus su jų elektrokataliziniu aktyvumu ant gryno Au, M/Ti ir M/TiO_2nv elektrodų. Natrio borohidrido oksidacijos srovės tankio vertės, išmatuotos ant Au(M)/Ti su nusodinto Au įkrova nuo 0,9 iki 57,6 $\mu g_{Au}\,cm^{-2}$ ir Au(M)/TiO_2nv katalizatorių su nusodinto Au įkrova nuo 8,2 iki 59,4 $\mu g_{Au}\,cm^{-2}$ yra apie 7-16 kartų yra didesnės nei ant gryno Au elektrodo. Didžiausiu masės aktyvumu (140 $mA\,\mu g_{Au}^{-1}$) natrio borohidrido oksidacijos reakcijai pasižymėjo Au(Ni)/Ti katalizatorius, su nusodinto Au kiekiu 0,9 $\mu g_{Au}\,cm^{-2}$. Taip pat nustatyta, kad išmatuotas

didžiausias $NaBH_4$-H_2O_2 kuro elemente prototipo galios tankis 25 ºC temperatūroje yra 224,3 mW cm^{-2}, panaudojant Au(Co)/Ti katalizatorių su nusodinto Au įkrova 57,6 µg cm^{-2}, o specifinis galingumas yra 102,6 mW μg_{Au}^{-1}, panaudojus kaip anodą Au(Ni)/Ti katalizatorių su nusodinto Au įkrova 0,9 µg cm^{-2}.

Suformuoti Au(M)/Ti ir Au(M)/TiO_2nv katalizatoriai yra perspektyvios medžiagos ir gali būti naudojamos kaip anodas tiesioginiuose natrio borohidrido kuro elementuose.

Information about the author

Name, surname	Aldona Balčiūnaitė
Birth date and place	15th of January 1988, Vištytis, Lithuania
Education 01/09/2006 - 30/06/2010	
2006-2010	Bachelor degree of Chemistry, Vilnius University
2010-2012	Master degree of Chemistry, Vilnius University
2012-2016	Doctoral studies at Institute of Chemistry of Centre for Physical Sciences and Technology
Work experience	
From 2013	Junior Research Assistant, Institute of Chemistry of Centre for Physical Sciences and Technology
2010-2012	Engineer, Institute of Chemistry of Centre for Physical Sciences and Technology

Informacija apie autorių

Vardas, pavardė	Aldona Balčiūnaitė
Gimimo vieta ir data	1988 01 15, Vištytis, Lietuva
Išsilavinimas	
2006-2010	Chemijos bakalauro laipsnis, Vilniaus Universitetas
2010-2012	Chemijos magistro laipsnis, Vilniaus Universitetas
2012-2016	Doktorantūros studijos, Chemijos institutas, Fizinių ir technologijos mokslų centras
Darbo patirtis	
Nuo 2013	Jaunesnioji mokslo darbuotoja, Chemijos institutas, Fizinių ir technologijos mokslų centras
2010-2012	Inžinierė, Chemijos institutas, Fizinių ir technologijos mokslų centras